Accepted Manuscript

Integrated U-Pb zircon and palynological/palaeofloristic age determinations of a Bashkirian palaeofjord fill, Quebrada Grande (Western Argentina)

Victoria Valdez Buso, Mercedes di Pasquo, Juan Pablo Milana, Benjamin Kneller, Claus Fallgatter, Farid Chemale Junior, Paulo Sérgio Gomes Paim

PII: S0895-9811(16)30326-1

DOI: 10.1016/j.jsames.2016.12.009

Reference: SAMES 1638

To appear in: *Journal of South American Earth Sciences*

Received Date: 8 January 2016

Revised Date: 9 December 2016

Accepted Date: 14 December 2016

Please cite this article as: Buso, V.V., di Pasquo, M., Milana, J.P., Kneller, B., Fallgatter, C., Junior, F.C., Gomes Paim, P.S., Integrated U-Pb zircon and palynological/palaeofloristic age determinations of a Bashkirian palaeofjord fill, Quebrada Grande (Western Argentina), *Journal of South American Earth Sciences* (2017), doi: 10.1016/j.jsames.2016.12.009.

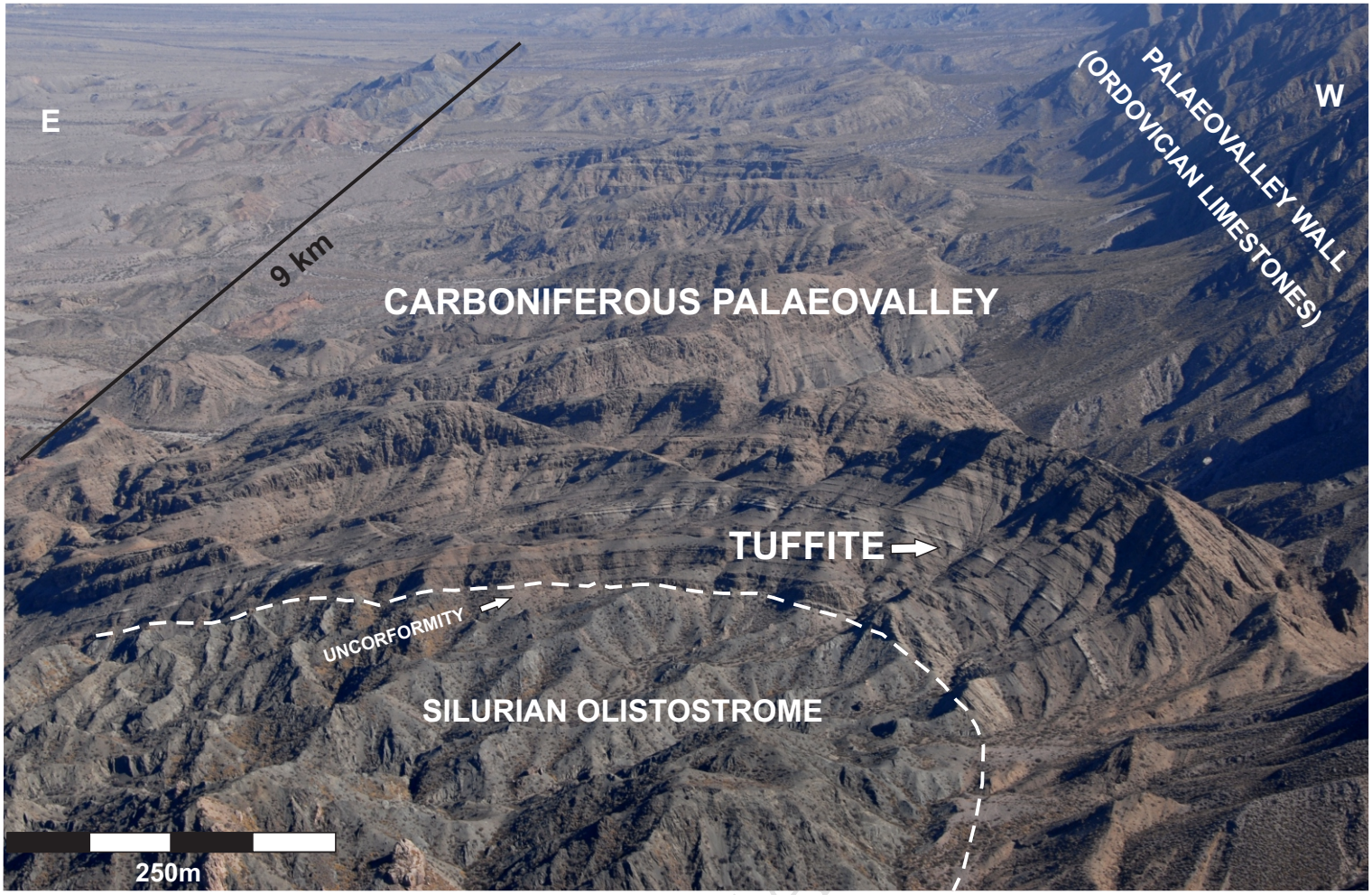
E
9 km
CARBONIFEROUS PALAEOVALLEY
W
PALAEOVALLEY WALL
(ORDOVICIAN LIMESTONES)
TUFFITE
UNCORFORMITY
SILURIAN OLISTOSTROME
250m


1.1
2.1
3.1
4.1
5.2
5.1
6.1
7.1
10.1
12.1
9.1
11.1
8.1
321.3 Ma
500 µm
CPGEO
HV
20.00 kV
WD
22.4 mm
spot
6.0
vac mode
High vacuum
mag
89 x

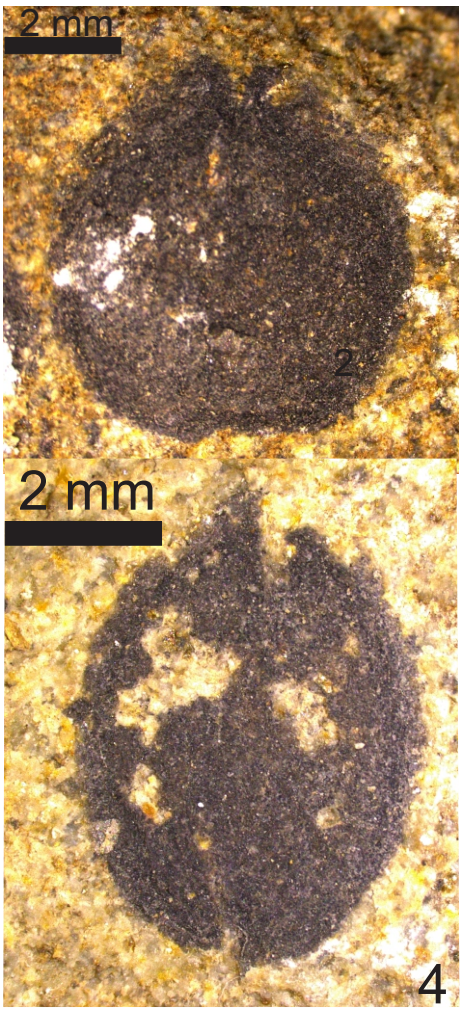
2 mm
2
2 mm
4

ESSENTIAL TITLE PAGE INFORMATION

Title:

Integrated U-Pb zircon and palynological/palaeofloristic age determinations of a Bashkirian palaeofjord fill, Quebrada Grande (Western Argentina)

Victoria Valdez Buso[1,4], Mercedes di Pasquo[2], Juan Pablo Milana[3], Benjamin Kneller[4], Claus Fallgatter[1], Farid Chemale Junior[1], Paulo Sérgio Gomes Paim[1]

Affiliation:

VICTORIA VALDEZ BUSO[1]

[1] UNISINOS - Universidade do Vale do Rio Dos Sinos, Programa de Pós-Graduação em Geologia. Av. Unisinos, 950, Cristo Rei, São Leopoldo, Rio Grande do Sul, Brasil, CEP 93022-000. E-mail: vikivaldezbuso@gmail.com

Corresponding author present address:

[4] Department of Geology and Petroleum Geology, School of Geosciences, University of Aberdeen, Aberdeen AB24 3UE, United Kingdom. E-mail: victoria.valdezbuso@abdn.ac.uk

MERCEDES DI PASQUO[2]

[2]CONICET - Consejo Nacional de Investigaciones Científicas y Técnicas Address: Laboratorio de Palinoestratigrafía y Paleobotánica, CICyTTP-CONICET, Dr. Materi y España S/N, Diamante (E3105BWA), Entre Ríos, Argentina E-mail: medipa@cicyttp.org.ar

JUAN PABLO MILANA[3]

[3]CONICET - Consejo Nacional de Investigaciones Científicas y Técnicas, Facultad de Ciencias Exactas Físicas y Naturales. Universidad Nacional de San Juan, Argentina. Av. Ignacio de la Roza 590(O), Complejo Universitario "Islas Malvinas", J4502DCS Rivadavia, San Juan, Argentina. E-mail: jpmilana@gmail.com

BENJAMIN KNELLER[4]

[4] Department of Geology and Petroleum Geology, School of Geosciences, University of Aberdeen, Aberdeen AB24 3UE, United Kingdom. E-mail: b.kneller@abdn.ac.uk

CLAUS FALLGATTER[1]

[1] UNISINOS - Universidade do Vale do Rio Dos Sinos, Programa de Pós-Graduação em Geologia. Av. Unisinos, 950, Cristo Rei, São Leopoldo, Rio Grande do Sul, Brasil, CEP 93022-000. E-mail: claus.geologia@gmail.com

FARID CHEMALE JUNIOR

[1] UNISINOS - Universidade do Vale do Rio Dos Sinos, Programa de Pós-Graduação em Geologia. Av. Unisinos, 950, Cristo Rei, São Leopoldo, Rio Grande do Sul, Brasil, CEP 93022-000. E-mail: faridchemale@gmail.com

PAULO SÉRGIO GOMES PAIM[1]

[1] UNISINOS - Universidade do Vale do Rio Dos Sinos, Programa de Pós-Graduação em Geologia. Av. Unisinos, 950, Cristo Rei, São Leopoldo, Rio Grande do Sul, Brasil, CEP 93022-000. E-mail: ppaim@unisinos.br

Abstract

This work presents a new age framework for the main Bashkirian glacio-eustatic transgression in Argentina, including the first absolute age for the Jejenes Formation, San Juan Province, based on radiometric dating of a crystal-rich tuff, supported by palynological and palaeofloristic studies, and presented within a revised palaeogeographic setting. The Jejenes Formation represents the glacial to postglacial fill of the Quebrada Grande palaeofjord carved in the Eastern Precordillera. The succession has been subdivided into five stages, the youngest of which suggests a previously unrecognised glacial event for this locality. Six productive levels for palynology were found within proglacial strata, and in the base and top of the succeeding interglacial stage. Palynoassemblages are characterized by poorly preserved trilete spores and monosaccate pollen grains along with a large amount of terrestrial phytoclasts. Main species indicating the *Raistrickia densa-Convolutispora muriornata* SubZone (DMa SZ) are *Vallatisporites ciliaris, Cristatisporites rollerii, C. stellatus, C. chacoparanensis, C. inconstans* and monosaccates such as *Circumplicatipollis plicatus.* This DMa SZ is estimated as Serpukhovian/Bashkirian and characterizes the glacial-related Guandacol Formation and equivalents units of the western Paganzo Basin. A tuffaceous level in in the proglacial unit, bearing platyspermic seeds, plant remains and palynomorphs, yielded first-cycle volcanic zircons that were analysed by SHRIMP. An absolute age of 321.3±5.3 Ma confirms a Bashkirian age for the main postglacial transgression in the Paganzo Basin, and offers a novel calibration for the palynoassemblages of DMa SZ that occurs elsewhere in Western Argentina.

Keywords: Late Palaeozoic Ice Age; Palynology; Platyspermic seeds; isotopic age; Jejenes Formation; Paganzo Basin

1. Introduction

The Late Palaeozoic Ice Age (LPIA) is probably the most important glacial period during the Phanerozoic (Veevers and Powell, 1987; Frakes et al., 1992; Isbell et al., 2003; Fielding et al., 2008), when different regions of Gondwana were affected by at least three diachronous glacial events (López Gamundí et al., 1997; Isbell et al., 2003). The first of these (Late Devonian-Tournasian) is only recorded in the Brazilian Solimões and Amazonas basins (Caputo, 1985) and in the Titicaca region of Bolivia (Díaz Martínez and Isaacson, 1994). The second glacial event (Serpukhovian-Bashkirian) is recorded in the Tarija Basin of Bolivia (e.g., Starck et al., 1993; Schulz et al., 1999; Azcuy and di Pasquo, 2000; Suárez Soruco, 2000; di Pasquo, 2003; Starck and del Papa, 2006; del Papa and di Pasquo, 2007; Isaacson et al., 2014) and in the Calingasta-Uspallata (González, 1981; González, 1990; López Gamundí, 1997; López Gamundí and Martínez, 2000; Henry et al., 2010), Paganzo (Limarino and Gutiérrez, 1990; López Gamundí and Martínez, 2000; Limarino et al., 2002; Pazos, 2002; Marenssi et al., 2005) and Río Blanco (Gulbranson et al., 2008) basins of western Argentina (Fig.1.A). The third glaciation (Late Bashkirian-Asselian) took place in different basins in the southeastern region of South America, Antarctica, South Africa, India and the western basins of Australia (Isbell et al., 2003; Fielding et al., 2008). In South America, these glacial events were characterized by periods of almost no sedimentation in the hinterland, when glaciers were at their maximum extent. Proglacial sedimentation took place during subsequent glacier retreat and ensuing postglacial transgressions, as recorded by the establishment of lakes and fjord embayment accompanied by climatic amelioration (e.g., López Gamundí, 1989; Buatois and Mángano, 1994, 1995; Limarino et al., 2002).

Late Palaeozoic basins in western Argentina record two glacial stages and subsequent transgressions (López Gamundí et al., 1992; Limarino et al., 2002, 2014; Limarino and Spalletti, 2006). The first one and ensuing transgression (preceding the main Serpukhovian/Bashkirian event), is recorded in few places in western Argentina (López Gamundí et al., 1992; Limarino et

al., 2002), and seems less important than the following stage judging by the amount of associated glacial and paraglacial sediments. It is the second glacial interval that comprises the main glacial diamictite units, and in many cases, they sole deep palaeovalleys excavated by glaciers up to 1 km deep below the crest of the valley walls in the Precordillera (Milana and Bercowski, 1990; López Gamundí and Martínez, 2000; Kneller et al., 2004; Dykstra et al., 2006). Thermochronometric studies of Late Palaeozoic palaeovalley deposits compared to their basement host, suggests these valleys were ca. 2 km deep in Sierras Pampeanas, the hinterland (Enkelmann et al., 2014) Therefore, all the evidence suggests that the second interval caused the largest recycling of previous deposits, except in pericratonic basins such as in the Río Blanco and Calingasta regions where higher rates of subsidence allowed partial preservation of the previous glacial sediments (e.g., Milana et al., 2014).

The Serpukhovian/Bashkirian transgression that marks the termination of the second glacial event is well documented in Huaco, Quebrada de Las Lajas, Quebrada Grande, and also in the Western domain of the Sierras Pampeanas, amongst other places (e.g., Guandacol Hill and Cerro Bola area, Valdez et al., 2013, 2015). Only few contributions have described another glacial event subsequent to this main Serpukhovian/Bashkirian transgression (Gulbranson et al., 2010; Valdez et al., 2013, 2015; Aquino et al., 2014), and there is not agreement if it could be a secondary event associated to the Serpukhovian/Bashkirian glaciation or if it can be considered a separate glaciation. In this context, this work focuses on the interval between the Serpukhovian/Bashkirian postglacial transgression in the Jejenes subbasin and the interglacial turbidites just before the third and locally the last glacial interval. This is the second record of a third glacial event after the main Serpukhovian/Bashkirian one from the Precordillera region (cf. Aquino et al., 2014).

The object of this study, the Jejenes Formation (located in the Eastern Precordillera, San Juan Province, Argentina), consists of ca. 250 m fill of a palaeovalley succession carved both into Ordovician limestones of the San Juan Formation, and the Ordovician-Silurian Rinconada

Formation, a *melánge* that includes kilometre-scale olistoliths of San Juan Formation. Sedimentary processes and their interpretations within this palaeovaley were described in detail by Kneller et al. (2004).

Concerning the age of the Jejenes Formation, palynological and paleobotanical information mainly from Quebrada de Las Lajas was published by González Amicón (1973), Gutiérrez and Césari (1987), Leguizamón and Vega (1990), Vega (1995), Brea and Césari (1995), Césari and Bercowsky (1997), Cladera et al. (2000), and Pujana (2005). The architecture of the fill of this palaeovalley was studied in detail by Dykstra et al. (2006).

For the present study an extensive and detailed survey and sampling was carried out in Quebrada Grande from 2012 to 2014, in order to find fossiliferous horizons and to characterize the palynofacies associations of the entire succession. In this contribution, we present the recovery of a taphoflora with lycophyte stems and the first platyspermic seed recorded from this region, as well as variably preserved stems and wood fragments. The recovery of several palynomorphs from different productive horizons and the possibility to date first cycle crystals recovered from a tuffite, allowed secure correlations with other stratigraphic units of the Paganzo basin. Additionally, a palynofacial analysis was carried out to improve palaeoenvironmental interpretation.

2. Geological setting

2.1. Regional setting

The Paganzo Basin, located in northwestern Argentina (Fig. 1.A), preserves extensive Mississippian and Pennsylvanian deposits related to Gondwana glaciation, with glacigenic successions, including proglacial strata such as mudstones with dropstones tillites, but also resedimented diamictites, and varves forming rhythmites (Limarino and Gutiérrez, 1990; López Gamundí and Martínez 2000; Marenssi et al., 2005). These strata are exposed in outcrops of

Guandacol Formation and its equivalents, such as the Jejenes Formation, which was defined as the fill of the Jejenes sub-basin, located in the southeast portion of the Paganzo Basin.

In the Precordillera area, sedimentation was initially controlled by the negative palaeorelief generated during the glaciation, and related successions take the form of isolated valley fills. Several paleovalleys with glacigenic strata are exposed in the Precordillera and adjacent areas (Milana, 1988; Milana and Bercowski, 1990; Astini et al., 1995; Kneller et al., 2004; Dykstra et al., 2006; Henry et al., 2010; Schatz et al., 2011; Aquino et al., 2014; Limarino et al., 2014). Also postglacial transgressive sediments have been identified in several localities (Limarino et al., 2002; Limarino and Spalleti, 2006). In this region, the transgression is recorded by marine facies in open fjord type environments (López Gamundí, 1987; Milana, 1988; Aquino et al., 2014) and rather more restricted fjord environments (Kneller et al., 2004: Dykstra et al., 2006).

Formerly, a mountain chain (the Protoprecordillera; Amos and Rolleri, 1965; Rolleri and Baldis, 1969) coincident with the modern Western Precordillera, was believed to separate marine settings to the west from purely continental settings to the east in the Upper Palaeozoic of the Central and Eastern Precordillera (Fig.1.B). In this paleogeographic scenario, the Maradonas sub-basin (Fig. 1.C) was interpreted as entirely continental, while to the west and along the western rim of Western Precordillera purely marine and glaciomarine deposits were ascribed to the Calingasta-Río Blanco basin. The Maradonas sub-basin is so called because the maximum thicknesses of Late Palaeozoic occurs near Maradonas in the Central Precordillera, 30 km south of the San Juan River valley. It formed part of the Paganzo basin and was limited to the west by the supposedly glaciated mountains of the Protoprecordillera. Glaciers were believed to radiate both east and west from the Protoprecordillera, and evidence of glaciomarine sedimentation to the west has been well known since DuToit (1930), with later depositional studies carried out by López Gamundí (1983) among others, while the palaeovalleys in this realm were defined by Milana and Banchig (1987) after correlating many detailed logs at Hoyada Verde. The hypothesis

of a Protoprecordillera was discussed in the light of the poor evidence by González Bonorino (1975), later supported as we show below.

Evidence found and published during the last 30 years clearly demonstrates that there was no barrier separating the western and eastern domains. The first evidence was shown by Milana et al. (1987) and Milana and Bercowski (1987a), who described a rich association of marine fossils including the typical Septosyringothiris sp (Lech et al., 1990), within a palaeofjord-estuary overlying the Devonian Punta Negra Formation (Milana, 1988), in the core of the Central Precordillera (Fig.1B). Further work in the area showed the presence of primary glacial deposits in almost all of the lower Paganzo beds exposed in the various thrust sheets of the Central Precordillera fold and thrust belt, and also the presence of glacial striated pavements in at least two of these thrust sheets (Milana and Bercowski, 1987b, 1990, 1993). Reconstruction of the topography by tracing glacial and postglacial marine deposits suggested an E-W orientation for the main glacial palaeovalley and west to northwest directed ice flow. The fjord could then turn south or north after hitting the eastern margin of the potential Protoprecordillera, but there is no evidence of glacial or marine deposits in either direction. Thus, all evidence from Central Precordillera points to ice outlet to the west and marine ingressions from the west, suggesting that any such Protoprecordillera did not form a barrier separating marine from continental basins. It also shows that glaciers were not coming from the west (except perhaps very locally for the case of the Jejenes Arch; Kneller et al., 2004), as all glacial flow indicated in the pavements of Central Precordillera at this latitude was towards the WNW. We suggest here the use of the term Tontal Arch (Cf. González Bonorino, 1975) to describe a chain of uplands dissected by glacial valleys, analogous to the fjordlands of southern Chile, as distinct from the continuous barrier to marine incursions implied by the term Protoprecordillera, hence our interpretation of the eastern palaeovalleys as fjords (Kneller et al., 2004; Dykstra et al., 2006).

However, the best evidence that there was no continuous barrier came from the discovery of marine deposits in what was supposed to be the core of Protoprecordillera. At least five levels

with marine fossils found in the Carboniferous sequence described in the Tontal range (Fig. 1.C), including glaciomarine sediments, suggest there was also a fjord developed in this area. Recent tectonics in this area have caused most deposits younger than lower to middle Palaeozoic to be eroded, except for erosive remnants whose paleontological content has been described in detail by Lech et al. (1998) and Lech and Milana (2006). Finally, the last evidence found suggesting that marine ingressions entered to the eastern Precordillera at the latitude of the San Juan River, was given by Aquino et al. (2014), who describe a marine palaeofjord at Talacasto gorge, in which southward directed palaeocurrents occur.

Given that the Jejenes Formation outcrops only occur on the east of the Eastern Precordillera range (the Zonda arch, Fig. 1. C), it could be interpreted that the Tontal arch formed a ridge limiting the marine ingressions, as is shown in some palaeogeographic maps (cf. Salfity and Gorustovich, 1983). This could be the case of Quebrada Grande palaeofjord as we found no evidence of Carboniferous sediments westward from the classical outcrops (cf. Kneller et al., 2004). However, this is not the case of the sediments filling the Quebrada de Las Lajas palaeofjord (Dykstra et al., 2006, 2011) which can be traced across the entire Eastern Precordillera, indicating that there were no limitations for marine transgressions to reach Jejenes Formation depositional area. Fully marine conditions were found only at the western rim of the Western Precordillera, and the Precordillera has been shortened by up to a 60% (Jordan et al., 1986), thus the Jejenes Formation depositional area was remote from open marine environments. The Eastern Precordillera would have been subject to the kind of oceanographic conditions seen in extensive modern fjord system such as in southern Chile, in which the surface layers have brackish waters (locally as low as 1 practical salinity unit; e.g. Sievers, 2008), and are locally hypoxic in the deeper waters (e.g. Silva & Vargas, 2014). This explains the absence of the normal marine fossil assemblages found in the Eastern Precordillera and scarce braquiopods found at the Central Precordillera, while similar eustatic evolution between Jejenes Formation, sequences and those of Central Precordillera imply a marine connection.

232 *2.2. Local setting*

233 The object of this study, the Jejenes Formation at Quebrada Grande, is exposed on the
234 eastern margin of the Sierra Chica de Zonda, in the foothills of the Eastern Precordillera, 25 km
235 south of the city of San Juan (Figs. 1 B, C and 2). It consists of ca. 250 m fill of a palaeofjord,
236 deposited during and just after the ending of the second main glacial episode
237 (Serpukhovian/Bashkirian). It cuts a steeply dipping Lower Palaeozoic succession (Fig. 3.A).
238 consisting of Ordovician platform limestones of the San Juan Formation (Beresi and Bordonaro,
239 1985), overlain to the east by an Ordovician-Silurian olistostrome (Rinconada Formation, Amos,
240 1954; Peralta, 1990; Peralta et al., 1994) consisting largely of highly deformed siliciclastic
241 turbidites, but including olistoliths of San Juan Formation limestone. The preserved exposures of
242 Jejenes Formation are about 1 km wide and 9 km long (Figs. 2 and 3A, B) with two possible
243 feeding arms, one sourced from the south and the main one sourced from the east as suggested by
244 most palaeocurrents of the main depositional Stage IV (cf. Kneller et al., 2004). Sedimentary
245 processes and their interpretations within this palaeovalley were described in detail by Kneller et
246 al. (2004).

247 The succession has been subdivided into five stages (Kneller et al., 2004, and this work):
248 Stage I contains massive and crudely stratified diamictites interpreted as subglacial deposits.
249 Stage II yields water-laid sandstones related to shallow-water deltas developed on the valley
250 floor. Stage III comprises gravel-rich subaqueous outwash fan facies encroaching down basin
251 with dropstone-bearing, basin-floor mudstones and turbidite sandstones, including a few tuffites.
252 Stage IV encompasses dropstone-free sandy turbidites. Finally, Stage V is composed of
253 proglacial mass-transport complexes and turbidite deposits, including erratic boulders and
254 outsized clasts (dropstones) that suggest a new glacial event for this locality.

255 Some palynological studies from Late Palaeozoic units cropping out on the eastern
256 margin of the Sierra Chica de Zonda (San Juan Province) have previously been published (Las
257 Crucecitas-del Agua river by González Amicón, 1973; La Mina creek by Gutiérrez and Césari,

1987; and Las Lajas creek by Césari and Bercowski, 1997). Taphofloras of compressions / impressions and wood fragments recovered from the Jejenes Formation were attributed to the Pennsylvanian NBG Zone (Fig.4) (Leguizamón and Vega, 1990; Vega, 1995; Brea and Césari, 1995; Cladera et al., 2000; Pujana, 2005). More detailed palynological and paleobotanical surveys of Serpukhovian-Bashkirian equivalent units of the Paganzo Basin (Fig. 4) were summarised by Azcuy et al. (2007), Césari et al. (2007), and Limarino et al. (2014). A South American biostratigraphic and stratigraphic correlation chart, including the NBG and DM Zones (Césari and Gutiérrez, 2001) and the Jejenes Formation, was proposed by Azcuy et al. (2007). The chronological position of both DM and NBG Zones (Fig. 4) was discussed by Césari et al. (2011) based on isotopic data from the Paganzo Basin (Gulbranson et al., 2010).

3. Material and methods

3.1. Geological survey and Palaeontology

Detailed fieldwork in Quebrada Grande revealed new geological evidence such as: 1) the recognition of glacial evidence in Stage V; and 2) the recovery of extensive and novel paleontological data. A tuffite previously described by Kneller et al. (2004), and related to the same interval (outcrop of Log 4, Fig. 5) plant fossils and palynomorphs, were analysed and dated. Other fossils such as stems, wood fragments and ichnofossils were also sampled and stored for future studies (Figs. 5 and 6).

In order to characterize the palynofacies associations of the entire succession, a systematic sampling was undertaken at the most prospective stratigraphic levels along the entire palaeofjord fill. Thirty six samples (mostly grey and green siltstones to very fine-grained sandstones) were collected from sedimentary logs measured in the northern, central and southern sectors of Quebrada Grande. Only Stages III and IV of the entire section yielded palynomorphs (Figs. 5 and 6); samples from Stages II and V were barren.

These samples were processed at the Laboratory of Palynostratigraphy and Palaeobotany in the Research Centre at Diamante, Entre Ríos (Centro de Investigaciones Científicas y Tecnológicas de Transferencia a la Producción: CICYTTP-CONICET). A standard methodology of maceration with HCl and HF was applied successively after reaching neutralization each time with several washes with distilled water (time of settling not less than 8 hrs.). Once the organic residue was recovered, it was boiled in HCl and washed up to neutralization in a centrifuge, and sieved to 25 µm. Palynological slides were mounted with jelly glycerine to perform the first analysis under the microscope, to define whether samples were productive or barren. Additionally, other treatments were performed to improve the potentially productive residues mounted in the same way (i.e., second HF, oxidation with HNO_3, concentration with ClZn; see Traverse, 2007). The palynological analysis was done under a light microscope Leica DM500 and a video camera Leica EC3 (3.0 Megapixels). All collected macrofossils (plants and trace fossils) and palynofossils are housed in the collections at CICYTTP (di Pasquo and Silvestri, 2014). Macrofossils were carefully cleaned and illustrated with a Panasonic Lumix DMC-ZS7 (12 Mp) digital camera and under a Leica stereoscope 58APO with a video camera Leica DFC 295 (5 Mp) at CICYTTP.

The constitutive elements (palynomacerals) of the sedimentary organic matter (kerogen) here identified are in agreement with Tyson (1995) and Batten (1996) as follows: phytoclasts (traqueids, cuticles), opaques (non-structured brown and black debris), amorphous organic matter (AOM), and palynomorphs. The characteristics and size of palynomacerals and the presence of pyritization of palynomorphs as well as their relative abundances are shown in Table 1 and Figure 7.

A biostratigraphic analysis of the palynoassemblages to establish their ages and correlation to other stratigraphic units of several other South American basins (Fig. 4) is based on the stratigraphic distribution of the species (Fig. 6) and their ranges, along with the known ranges of the species of platyspermic seeds as well as the isotopic data discussed below.

3.2. Geochronology: Acquisition and data processing

U-Pb zircon analysis from one tuffite sampled in the upper Stage III (outcrop in Log 4, Fig. 5) was carried out at the Laboratory of High Resolution Geochronology of the Institute of Geosciences of University of São Paulo (GeoLab-IGc-USP) using SHRIMP IIe equipment. About 1 kg of rock was sampled from the bed for petrographic and geochronological studies. U-Pb SHRIMP zircon preparation was done by hand picking zircon grains that were extracted by standard crushing, milling, then sieving (0.150 – 0.063 mm), Wiffley table, and heavy liquid techniques (bromoform - density = 2.85, and methylene iodide - density = 3.32). Five to seven fractions (magnetic to nonmagnetic) were separated using the Frantz magnetic barrier separator and after removing ferromagnetic minerals with a hand magnet. After getting the final concentrate of minerals, zircon grains were selected manually according to their crystallinity with a stereo microscope and a micro-gripper. Handpicked zircons were mounted in epoxy discs along with zircon standards (Temora 2), ground and polished, microphotographed in transmitted and reflected light, and imaged using scanning electron microscope (backscattered electrons – BSE) and cathode luminescence. Mounts were then cleaned and gold-coated in preparation for SHRIMP analysis. Analytical procedures and data treatment follow the methods presented by Sato et al. (2014). Zircon grains were analysed with a 2-3nA, 10kV primary O2- beam focussed to a ~ 30μm diameter spot with a beam density around 2.5-7 ηA (dependent on brightness aperture). At mass resolution between 5000 and 5500 the Pb, Th and U isotopes were resolved from all major interferences. Reduction of raw data and age calculation were carried out using Squid 1.06 and Isoplot-Ex (Ludwig, 2008). U and Th concentrations were determined relative to those measured in the standard SL13 and Temora 2 was used to calculate the $^{206}Pb/^{238}U$ age.

4. The Quebrada Grande palaeofjord fill

The palaeovalley fill represents the interplay between sea-level rise, glacial retreat and the resulting changes in sediment supply and depositional processes. Below is a summary of Kneller

et al.'s (2004) descriptions and interpretations of their five stages of the palaeofjord fill although Stage V is here re-interpreted as a new glacial episode.

-Stage I (glacial deposits): consists of lodgement and flow tills, representing an ice-filled valley. They include massive diamictites having a green, silty mud matrix and crudely stratified matrix-supported gravels. They are interpreted as having been deposited primarily by ice (lodgement till). Stage I deposits may reach up to 13 m thick and occur in the palaeo-lows of the palaeovalley.

-Stage II (shallow-marine deposits): includes a shallow water delta on the valley floor and represent initial flooding of a partially open valley. They consist of waterlain, laminated and cross-laminated sandstones overlying Lower Palaeozoic basement or glacially-related diamictites of Stage I. A range of subaqueous facies was deposited during the rise of base level, the early part of which may have been lacustrine, and was locally accompanied by the formation of shallow-water deltas on the valley floor. These were rapidly drowned to a depth of 100 meters or more, initiating the deep-water succession (Stage III).

-Stage III (proglacial, deepwater deposits and maximum flooding interval): encompasses gravelly outwash fan deposits, basin floor turbidites and black shales, representing a flooded valley, with local tributary glaciers. This gravel, sand- and mud-rich succession was fed by subaqueous glacial outwash and associated plumes, with floating ice providing ice-rafted debris. Dropstones are numerous in the lower part of the succession, and overall become less abundant upward. According to Kneller et al. (2004) three thick, correlatable tuffites (T0 to T2) occur within transgressive shales and mudstones forming the upper part of Stage III (Fig. 6). The tuffites form distinctive, whitish, normally graded beds of altered, crystal-rich tuff. The lowermost tuffite T0 (here named QG tuffite) was selected for geochronological studies due to its stratigraphic position and low grade of detrital contamination, which is suggestive of a primary volcanic origin. Wood and leaf fragments are especially common just below the analysed tuffite although

leaf debris also occur within the tuffite. A good collection of lycophyte stems, platyspermic seeds and palynomorphs was recovered from this interval (Fig. 6).

-Stage IV (sandy turbidites): consists of a ≤ 100 m thick turbidite sand sheet system. It is composed of thin to very thick bedded, ungraded to normally graded sandstones with thin mudstone or siltstone caps with plant debris. Turbidites display partial or complete Bouma sequences.

-Stage V (proglacial, mass-transport deposits and turbidites): consists of a 90 m thick package of turbidites, mass transport and fan delta deposits (Fig. 8). This unit starts with massive to stratified, up to 20 m thick conglomerate with an erosional contact with the underlying Stage IV. In some places, the lower interval of the conglomerates contains outsized, up to 4 meters striated boulders of granites and metamorphic rocks embedded in a poorly-sorted conglomerate that includes well-bedded, clast-supported conglomerates as well as massive, pebbly sandstones (Figs. 8 and 9 A-D). The succession continues with slumped deposits. The upper part of Stage V consist of two heterolithic intervals characterized by thin-bedded, rippled sandstones intercalated with siltstones with dropstones (Fig. 10 A-D) overlain by a matrix- to clast-supported conglomerate interpreted as a debris flow deposit.

5. Results

5.1. Petrography of the tuffite sampled for geochronology

Thin sections of the dated tuffite suggest a resedimented acid tuff, or tuffite, composed of devitrified shards (vitroclasts), crystals and lithic fragments (Fig. 11), all of them contained in a very fine volcanic matrix. Shards range from ash to very fine ash size (fragments ≤1 mm), are angular and cuspidal, and generally colourless, suggesting an acid composition. Crystals are smaller than 1 mm, and composed of quartz, alkali feldspar and plagioclase, in decreasing order of abundance. They exhibit angular to rounded, and subhedral to anhedral shapes. Fractures are common and indicative of rapid cooling. Crystal composition corroborates an association with

383 acid volcanism. Lithic fragments are extremely varied, consisting of tuffs and tuff powder, and
384 rarer small sedimentary (probably siltstones) and metamorphic (gneiss and/or quartzite) rock
385 fragments.

386 *5.2. Geochronology*

387 Twelve prismatic zircons from the tuffite sample were analysed (Fig. 12). Two
388 populations were distinguished: (i) three zircons yielded ages from 1088 ±24 to 1204 ±32 Ma
389 (8.1, 9.1, 11.1), and (ii) nine zircon grains yielded ages from 347 ±8.4 to 311 ±7.2 Ma. One
390 zircon of the second population was dated at centre and margin (spots QG-5.1 and 5.2). The U-
391 Pb isotope data for the twelve analysed zircon grains are summarized in Table 2 and cathode-
392 luminescence images of all zircons with spot locations are shown in Figure 12. The mean
393 $^{206}Pb/^{238}U$ age calculated from the seven concordant younger zircon grains is 321.3 ±5.3 Ma
394 (number of spots = 8) with a mean square weighted deviation (MSWD) = 0.71 (Fig. 13). This
395 corresponds to early Bashkirian according to the timescale of Cohen et al. (2013).

396 *5.3. Palaeobotany*

397 A taphoflora and palynological data were recovered from the same level as the dated
398 tuffite (Figs. 5, 6). Most of the plant remains documented are lycophyte stems and platyspermic
399 seeds (Fig. 14) preserved in the muddy section below the tuffite, within the tuffite and in the
400 sandy turbidites (Fig. 15 A-F). A detailed taxonomic analysis of the whole collection of
401 macro/mesofossils from this area is beyond of the scope of this contribution. Of these, the
402 indeterminate lycophyte here illustrated (Fig. 14.A) is an example of the herbaceous stems found
403 in this deposit and preserved as impressions and compressions in whitish grey siltstones and
404 yellow fine-grained sandstones. It is characterized by roughly rhomboidal leaf cushions (false
405 leaf scars) that exhibit a lepidodendroid phyllotaxy with orthostichies and horizontal lines clearly
406 visible. It is similar to *Frenguellia eximia* (Frenguelli) Arrondo et al. 1991 (known from the
407 Visean – Serpukhovian – Bashkirian of South America) and *Malanzania starckii* di Pasquo 2009

(from the Bashkirian-Moscovian Tarija Formation, Salta Province, Argentina). However, the lack of leaves in this specimen (among others) prevents its taxonomical assignment to one of those species, which are mainly distinguished on the grounds of their leaves (i.e., pentafurcated vs. simple tips respectively; Gutiérrez and Arrondo, 1994).

The platyspermic seeds are the first recorded in this region, and due to their biostratigraphic importance related to a specific age level they are further described.

Cordaicarpus Geinitz, 1862 emend. Archangelsky, 2000

Type species. *Cordaicarpus cordai* Geinitz, 1862 ex Seward, 1917

Cordaicarpus cesariae Gutierrez et al., 1992 emend. Archangelsky, 2000

Fig. 14 B

Description: Bilateral symmetry, subcircular shape, plane to rounded base, and a narrow sarcotesta (less than 1 mm), which is slightly expanded in the apical region, where it is also opened or broken. The sclerotesta shows an acuminated apex that does not project outside the sarcotesta. Although the overall size of the single specimen recorded and illustrated is small (ca. 6 mm in lenght and 5 mm in width), it is within the size range of the species.

Cordaicarpus famatinensis Gutierrez et al., 1992

Fig. 14.C, D

Description: Bilateral symmetry, longitudinally oval shape, rounded base, and a narrow sarcotesta (less than 1 mm), which more or less maintains its width up to the apical region. The latter ends sharply and it is frequently opened (or broken). The sclerotesta shows an acuminated apex that does not project outside the sarcotesta. The overall size of the two specimens illustrated is small (ca. 6 mm in length and 4.5 mm in width), but within the size range of the species.

Comparisons: The overall morphology of our specimens is in agreement with the original description of those species (Gutiérrez et al., 1992). *Cordaicarpus cesariae* differs from *C. famatinensis* in having the sarcotesta slightly widened to the apical part with round endings and being subcircular in shape.

5.4. Palynology

Eight productive samples yielded palynomorphs and they were found in the muddy section of Stage III (CICYTTP-PL 1049, 1054, 1053), and the mud caps of the turbidites of Stage IV (CICYTTP-PL 1051, 1055, 1062, 1056, Figs. 5 and 6). They are characterized by scarce to relatively frequent trilete spores (15 species) and very scarce to absent monosaccate pollen grains (3 species). It is noted that monosaccate pollen grains are recorded in small amounts from the lowest productive sample (CICYTTP-Pl 1049, Figs. 6, 14, 16). The general preservation of miospores is poor to rather good (CICYTTP-Pl 1056, 1062), the thermal alteration index (TAI in Utting and Wielens, 1992, Fig. 7) is high and ranges between 3 (dark black) and 4 (dull black), suggesting that the sediments reached the dry gas generation zone. Another six samples yielded exclusively variable proportions of phytoclasts and opaques, and AOM is present in four of the 13 levels analysed (Figs. 7, 16 and Table 1). The qualitative palynofacies information of the samples obtained from Stages III and IV are described as follows:

Palynofacies from Stage III: Four samples were recovered, of which three levels yielded a low abundance of palynomorphs (1-3%) and a high abundance of opaques (60-80%) and less phytoclasts. Both opaques and phytoclasts are mainly equidimensional in shape, although bladeshaped (B) and angular (A) forms are also present in variable sizes (i.e. poor sorting). Palynomorphs are mostly represented by dark brown, poorly preserved spores such as *Cristatisporites stellatus, C. inordinatus, C. menendezii*. Scarce and indeterminate monosaccate pollen grains were present in sample CICYTTP-Pl 1049. A tuffite occurs within this stage as a distinctive, whitish, normally-graded bed of altered, crystal-rich tuff. Wood fragments are especially common below and within the tuffite. A good collection of plant fossils, especially

456 lycophyte stems and platyspermic seeds, and one sample with palynomorphs were collected
457 (CICYTTP-Pl 1053). The other sample CICYTTP-Pl 1052 of this deposit yielded exclusively
458 finely fragmented, well sorted, black and brown particles, usually bladeshaped (B) and rare
459 angular (A) fragments.

460 Palynofacies from Stage IV: Nine samples were recovered containing kerogen. Five of them
461 exhibit only phytoclasts and opaques and one presents a low AOM content (Fig. 7). Four yielded
462 palynomorphs and interestingly, in the three first samples following the stratigraphic order (Fig.
463 6), pyrite is present in both palynomorphs and phytoclasts in its framboidal and euhedral forms
464 (Figs. 7, 16). Sample CICYTTP-Pl 1051 comes from a section associated with plant stems whilst
465 CICYTTP-Pl 1055 and 1062 are from a heterolithic section where some lycophyte stems were
466 also found interbedded. Sample CICYTTP-Pl 1051 yielded very poorly preserved palynomorphs
467 (10%), and quite similar percentages of phytoclasts and opaques, mostly fragmented to small-
468 and medium-size particles (moderately sorted), mostly blade- and angular-shaped. Sample
469 CICYTTP-Pl 1055 is composed of 15% of spores, mostly represented by *Vallatisporites ciliaris*,
470 *Cristatisporites inconstans* and *Cristatisporites stellatus*, and very poorly preserved
471 (indeterminate, fragmented and corroded by pyritization) monosaccate pollen grains. Phytoclasts
472 dominated by traqueids and opaques occur in similar proportion. Most of these palynodebris are
473 fragmented and corroded, moderately sorted (small- and medium-size particles) and commonly
474 angular- and blade-shaped. A low AOM content is recorded. Sample CICYTTP-Pl 1062 is quite
475 similar to the latter although sorting of palynodebris is poor; *Cristatisporites scabiosus*,
476 *Lundbladispora braziliensis* and *Plicatipollenites malabarensis* are present and *Vallatisporites*
477 *ciliaris* is absent. The samples CICYTTP-Pl 1061 to CICYTTP-Pl 1057 are characterized only by
478 palynodebris. The latter level exhibits also a low AOM content. Some variations in size, sorting
479 and shape of the palynodebris are shown in the Figure 7. Sample CICYTTP-Pl 1058 differs from
480 the others on its composition characterized by well sorted, large and blade-shaped traqueids and
481 black phytoclasts. No cuticles were observed. The last productive sample, CICYTTP-Pl 1056, is

similar to CICYTTP-Pl 1062, with the dominance of small and blade-shaped palynodebris, a low AOM content and the appearance of *Circumplicatipollis plicatus, Cannanoropollis trigonalis, Lundbladispora riobonitensis, Murospora torifera* and *Convolutispora muriornata* along with other species of the lower levels (Fig. 6).

6. Depositional model of Quebrada Grande palaeofjord

New field observations and palaeontological information here reported are integrated to improve the depositional model of the QG palaeofjord. Palynofacies assemblages provided some insight into the depositional conditions of stages III and IV.

Stage I represents glacial advance and minor sedimentation (Fig. 17.A). Lodgement tills occur as the fill of minor depressions cut into the valley floor, so they occur sparsely and very locally at the base of the Carboniferous succession (Kneller et al., 2004). Clasts in the tillites consist of Ordovician limestones and Precambrian basement rocks. The limestones clasts match the fractured carbonate lithology of the olistoliths within the Rinconada Fornation, and are thus derived from the local substrate. The basement clasts are dissimilar to any lithologies found within the Eastern Cordillera or any potential Protoprecordillera source to the west. They are, however, consistent with the very extensive basement outcrops of Sierras Pampeanas to the east of the Jejenes subbasin, and are thus consistent with ice caps being located on the craton.

Stage II marks the beginning of glacial retreat and resulting gradual flooding of the valley, but associated with a very high sediment input derived from the ice melting. Shallow water sandstones and conglomerates with NNW-dipping clinoforms represent the progradation of Gilbert-type deltas and associated delta-plain braided streams (Fig. 17.B). Stage II prograded into gradually deepening water of perhaps a few tens of meters depth. Because the valley floor may have lain considerably below the sill, the initial water body related to this stage may initially have been a restricted environment (Kneller et al., 2004).

Stage III records an acceleration of the ice melting and resulting extensive marine flooding. Gravelly subaqueous fans, dropstone-bearing basin-floor mudstones and thin-bedded turbidites represent this scenario (Fig. 17.C). Mudstones were probably deposited from buoyant plumes associated with the subaqueous meltwater discharge (Kneller et al., 2004). A volcanic event represented by the tuffite is confirmed by petrographic analysis and it was likely the responsible for the large accumulation of charred plants remains consisting of fragmented herbaceous stems and tiny seeds as well as rather poorly preserved palynomorphs. A rapid accumulation of ashes and fine clastic sediments is suggested that permitted their preservation. Samples CICYTTP-Pl 1054-1052 from this interval (Figs. 6, 7 and Table 1) are characterized by large amounts of phytoclasts that diluted the palynomorphs (Tyson 1995, p. 446; Batten, 1996, p. 1072). The presence of finely fragmented (well sorted) black and brown particles (mostly blade-shaped and less frequently angular fragments), especially in CICYTTP-Pl 1052, indicates a settling process. The upward-decreasing abundance of dropstones until their complete disappearance reflects the general retreat of floating ice as melting progressed. These strata may have been related to the establishment of a more open marine connection due to sustained transgression and were probably deposited from glacial meltwater plumes, iceberg rafting, and turbidity currents. The wood fragments especially common in the upper Stage III (Log 4 in Fig. 5, Fig. 6) are evidences of ice rafting into the basin.

The transition from lower to upper Stage III (Fig. 17.C and D) indicates a continued sea-level rise associated with glacier retreat. The maximum flooding interval occurs between the dropstone-free mudstones of upper Stage III (Fig. 17.D) and the sandy turbidites without dropstones of the base of Stage IV. This latter stage is represented by a 100 metre thick sequence of sheet sands ascribed to low and high-concentration turbidity currents. Sample CICYTTP-Pl 1051, from the basal turbidite deposits of the Stage IV (at outcrop of Log 9, Fig. 5), is associated with poorly preserved plant stems. Other fragments of plant material were found at the tops of sandstone beds in the interval corresponding to palynological sample CICYTTP-Pl 1062. The

samples between the latter levels and CICYTTP-Pl 1056 yielded exclusively phytoclasts as dominant components of organic matter in oxidizing environments, where palynomorphs are not present due to extreme dilution or they were selectively destroyed (see Tyson, 1995). The high abundance of phytoclasts in most of the samples (Table 1) indicates a fluvio-deltaic source and the presence of pyrite in palynomorphs found in the levels corresponding to the Stage IV (1051, 1055, 1062, see Table 1) supports deposition in marine environments. Pyritization of palynomorphs is normally associated with marine waters (with minor sources of high sulphate waters related to volcanic environments) where sulphate-reducing bacteria produce pyrite in the organic matter deposited under stable anoxic – dysoxic bottom conditions. Framboidal pyrite is associated with euxinic conditions where high organic matter content produces stratified water and the reaction of the bacteria is occurring in the water column as well (see further explanations in Mozer, 2010, and several references therein). Since the terrestrial palynomorphs recorded in these samples are transported, they could have been affected by pyritization in euxinic ponds prior to final deposition. In our case we interpret the pyritization of palynomorphs to have occurred after final deposition, because probably as they are so damaged they would not have resisted transport.

Concerning the maturation colour of the productive samples in Stage IV, they showed quite similar colour between medium to very dark brown (TAI ca. 3-4, Fig. 7), probably due to taphonomical processes prior to final burial in the depocenter and later diagenetic processes (see Batten, 1996). This is also supported by the poor preservation of scarce monosaccate pollen grains, and frequent fragmentation of the spores which along with pyritization in some intervals almost destroyed most of them (Fig. 16 and Table 1). The very low presence of well preserved cuticles in general and the dominance of black (?charcoal) particles may support this interpretation as well (Tyson, 1995).

Stage V facies rest on a main erosional surface cut into the turbidite sand sheets of Stage IV. The basal interval of Stage V is complex and display short distance facies changes recording

558 diverse depositional processes. Whereas in the northern part of the palaeovalley it comprises
559 matrix-supported conglomerates, in the central part it encompasses clast-supported, massive and
560 stratified conglomerates, occasionally including outsized clasts (Fig. 9). It is here suggested that
561 these erratic boulders are a sort of a residual lag related to the long term winnowing of a former
562 glacial deposit. Gravels deposited around erratic boulders seem non-cogenetic with them, as the
563 conglomerates show evidence of traction currents that would have been incapable of transporting
564 such outsized boulders. As a whole Stage V (Fig. 17.D) registers the development of fjord-head
565 deltas and fan deltas formed after a glacially-induced sea level fall, when sea-level rise was
566 surpassed by the deglacial sedimentary input. A subsequent transgression is recorded by
567 heterolithic, proglacial deposits including ice rafted debris (IRDs).

568 Concerning the floral composition of the assemblages recorded in Stages III and IV, they
569 are dominated by the lycophyte group represented in both macro and palynofossils, the latter
570 being represented by several genera such as *Cristatisporites, Vallatisporites, Kraeuselisporites,*
571 *Lundbladispora*. This group is ecologically related to the margin of water bodies and especially
572 humid environments (hydro-hygrophytic affinities) probably developed in the surroundings of
573 the marine setting. Scarce palynotaxa related to the ferns (e.g., *Convolutispora, Murospora*)
574 could have been the understory of the Cordaitean and Coniferalean (Gymnosperm) forest. The
575 former group of gymnosperms seems to have grown in the surroundings of the fresh water
576 paralic swamps or peats with lycophytes (Raymond et al., 2010), as they appear frequently in
577 association, such as in the tuffite interval (Fig. 6). Instead, the Coniferaleans are interpreted (like
578 modern forms) to have grown farther from standing water, in well drained soils of the margins of
579 valleys and in more elevated areas (e.g., DiMichele et al., 2010), and seem to have been better
580 developed in the uppermost Stage IV (Fig. 6). The observed assemblages are inherited from
581 primary depositional sites of these sediments, which were subsequently resedimented (along with
582 their assemblages of organic material) into deeper water by gravity flow processes (e.g.
583 hyperpycnites, turbidity currents).

7. Discussion

7.1. Age and correlation

The isotopic date here obtained from prismatic zircons of the tuffite indicates an absolute age of 321.3 ±5.3Ma. This absolute age corresponds to the earliest Bashkirian of the Global Time Scale (Cohen et al., 2013) and agrees with the relative age provided by the platyspermic seeds and palynoassemblages (Figs. 4-7 and Table 1), which are useful to evaluate the time interval of the postglacial succession of the QG palaeovalley. The platyspermic seed *Cordaicarpus cesariae* was recorded in the Pennsylvanian NBG Zone of the Agua Colorada, Tupe, Andapaico, Solca and Cerro Agua Negra formations of western Argentina (Gutiérrez et al., 1992). Balseiro et al. (2009) recorded the same species as part of a plant assemblage of the Loma de los Piojos Formation (southwest Jáchal, San Juan Province). This taphoflora bears plant species such as *Tomiodendron* and *Frenguellia eximia* that allowed the authors the definition of a new plant zone filling the Serpukhovian gap between the *Frenguellia–Paulophyton* zone (Mississippian) and the NBG zone (Pennsylvanian). However, its boundaries still need to be clearly defined, as well as the specific assignment of *Frenguellia eximia* as the five segments of the leaf were not clearly observed in their material as stated by Balseiro et al. (2009). Outside the Paganzo Basin, a single Pennsylvanian record of this species was documented by di Pasquo (2009) in the Tarija Formation of the Tarija Basin (Aguaragüe range, Salta Province, Argentina). It was attributed to the Bashkirian-Moscovian on the basis of the palynomorph species including monosaccate pollen grains characteristic of the BC Zone (di Pasquo 2003, 2007). *Cordaicarpus famatinensis* was documented in the Agua Colorada, Lagares, Tupe (Gutiérrez et al., 1992), and Guandacol (Gutiérrez and Pazos, 1994; Gutiérrez et al., 1995) formations of the Paganzo Basin. The platyspermic seeds are related to cordaiteans and primitive coniferaleans (Gutiérrez et al., 1992), which are known in the global record around the Mississippian / Pennsylvanian boundary (e.g., di Pasquo, 2002, 2009; Balseiro et al., 2009). The monosaccate pollen grains (e.g., *Plicatipollenites malabarensis, Circumplicatipollis plicatus*) are known of cordaitean-

coniferalean floral affinity. Their presence in the same section (Figs. 5, 6) confirms the correlation of the Jejenes Formation to the Serpukhovian-Bashkirian Subzone A of the *Raistrickia densa-Convolutispora muriornata* (DMa) Zone (César and Gutiérrez, 2001). The first record of pollen grains is documented in the Guandacol Formation and its correlatable units (e.g. lower Agua Colorada, Malanzán, Lagares and El Paso formations) from central-western Argentina (see César et al., 2011; Pérez Loinaze and César, 2012; Valdez et al., 2013; Vergel et al., 2015). Gulbranson et al. (2010) obtained a late Serpukhovian–Bashkirian minimum absolute age (ID-TIMS $^{206}Pb/^{238}U$ 319.57 ±0.09 Ma and 318.79 ±0.10 Ma) of the DMa SZone from postglacial transgressive facies of the Guandacol Formation just above their basal glacial deposits (César et al., 2011, p. 157). Hence, the assemblages bearing monosaccate pollen grains of the DMa Zone are constrained to an age not older than late Serpukhovian. This is also supported by the absence of monosaccate pollen grains in the underlying *Reticulatisporites magnidictyus-Verrucosisporites quassigobbetti* (MQ) Interval Zone from the Cortaderas Formation assigned to late Visean – early Serpukhovian (Pérez Loinaze, 2007).

Similar palynofloras outside the Paganzo Basin are documented in the early Bashkirian *Crassispora kosankei – Cystoptychus azcuyi* (KA) Zone of the Tupambi Formation (Fig. 4) from the Tarija Basin (Salta Province) in north-western Argentina and southern Bolivia (di Pasquo, 2002, 2003, 2007) and the early Pennsylvanian El Imperial Formation (San Rafael Basin) that records a glacial to postglacial transition at the Rio Atuel canyon (Mendoza Province, Fig. 4). In the latter, palynoassemblages with monosaccates were obtained from shales and siltstones of the middle part of the El Imperial Formation together with ichnofossils, which show degradation due to pyritization and yielded scarce acritarchs suggesting at least brackish-waters (rather than fresh-water conditions) in a fjord depositional system (Pazos et al., 2007).

7.2. The Stage V glacial advance

New observations made through the entire Stage V suggest a complex origin. In particular, it is very important to point out the presence of large boulders of composition that

636 does not fit the subcrop, so they cannot be the result of rock fall directly from the fjord sides,
637 even if there was still a large relief left at this stage of the palaeovalley fill. No evidence was
638 found to explain how a 4 m large boulder could be transported by the same mechanisms
639 associated with the first beds of Stage V. The most plausible interpretation is that boulders
640 dispersed along the base of Stage V are not genetically related to the surrounding beds. Basal
641 facies comprise crudely bedded, clast-supported to sandy conglomerates related to tractive
642 mechanisms that would not be able to transport boulders of several tons. In this context, boulders
643 sparsely found over the base of Stage V would be the fossil equivalent to present day "erratic
644 boulders", which are usually the erosive remnants of glacial drift. These boulders could also be
645 the remnants of large debris flow deposits later eroded. However, the several debris and mass
646 flow deposits found above the basal beds of Stage V did not carry any outsized boulder. This
647 point suggests glacial emplacement as drift and then turned into erratic boulders by subsequent
648 erosion of the finer material as the most likely mechanisms. The glacial/paraglacial nature of this
649 unit is reinforced by the reappearance of dropstones in the fine-grained, laminated units
650 preserved interbedded with the coarse-grained units.

651 Therefore, the presence of Precambrian basement outsized clasts through Stage V, either
652 as erratic boulders at its base or as dropstones within the heterolithic deposits, suggests a glacial
653 advance from the eastern Sierras Pampeanas and a discrete glacial pulse after the main
654 glaciations recognized elsewhere (Gulbranson et al., 2010; Aquino et al., 2014).

655 **8. Conclusions**

656 The analysis of the flora and palynoflora collected above, within and below the tuffite
657 (Stage III) and in the sandy turbidites (Stage IV) allowed the attribution of a Bashkirian age to
658 this part of the Jejenes Formation. A correlation to the *Raistrickia densa-Convolutispora*
659 *muriornata* Zone (DMa SZ) is proposed due to the occurrence of main species such as the
660 *Vallatisporites ciliaris, Cristatisporites rollerii, C. stellatus, C. chacoparanensis, C. inconstans*

and monosaccates such as *Circumplicatipollis plicatus*. In addition, the first platyspermic seed for the region is recorded in the same tuffaceous level that yielded an absolute age of 321.3 ±5.3 Ma. ($^{206}Pb/^{238}U$ SHRIMP analysis of first-cycle zircons).This radiometric dating confirms a Bashkirian age for the main postglacial transgression in the Paganzo Basin, and offers a novel calibration for the palynoassemblages of DMa SZ bearing monosaccate pollen grains that occur elsewhere in Argentina and Bolivia. The palynofacies analysis of the samples in Stage IV yielded palynomorphs with pyrite in their walls that support the interpretation of marine settings linked to the transgressive event. The palaeographic setting of the Jejenes Formation demonstrate there was no barrier to marine incursions into the area of these outcrops, and probably waters were not fully marine but mixed with fresh water from glacial sources or proglacial rivers, indicating that any uplands to the west ('Palaeoprecordillera') did not form a western barrier. Finally, a new local glacial event in the upper section of the Quebrada Grande area is recorded by the presence of erratic boulders and dropstones of Stage V. The Precambrian affinity of the outsized clasts (schist, metamorphic, granitic) suggests a possible ice advance and subsequent retreat from Sierras Pampeanas, located in the craton to the east.

Acknowledgements

This work is part of a research project supported by BG Brazil E&P Ltda. entitled "Carboniferous deglacial record in the Paraná Basin and its analogue in the Paganzo Basin of Argentina: Impacts on reservoir predictions" undertaken at the *Universidade do Vale do Rio dos Sinos* (UNISINOS), Brazil, in partnership with *Universidad Nacional de San Juan*, and University of Aberdeen, United Kingdom; and with funds from *Consejo Nacional de Investigaciones Científicas y Técnicas* CONICET PIP 0305 (2011-2013). This contribution is part of the PhD of the senior author funded by BG Brazil E&P Ltda. A special acknowledgment is made to Carla Puigdomenech, Carol Aquino, Deise Silveira, Fabiano Rodrigues and Willian Matsumura, who have collaborated during field work. To Professors Andrea Sander and Wilson Wilder, who helped with the petrographic analysis of the tuffite. Thanks are also given to Lic.

Leonardo Silvestri for his help in sample processing at the CICYTTP-CONICET. At last, the authors would like to acknowledge the ANP (Agência Nacional do Petróleo, Gás Natural e Biocombustível) and the Brazilian National Agency for Petroleum, Natural Gas, and Biofuels for their economic assistance.

List of species with authority mentioned in the text

Spores

Convolutispora muriornata Azcuy
Cristatisporites inconstans Archangelsky and Gamerro
Cristatisporites inordinatus (Menéndez and Azcuy) Playford
Cristatisporites menendezii (Menéndez and Azcuy) Playford emend. César
Cristatisporites rollerii Ottone
Cristatisporites scabiosus Menéndez
Cristatisporites spinosus (Menéndez and Azcuy) Playford emend. César
Cristatisporites stellatus (Azcuy) Gutiérrez and Limarino
Lundbladispora braziliensis (Pant, Srivastava) Marques Toigo, Pons emend. M. Toigo and Picarelli
Lundbladispora riobonitensis Marques Toigo and Picarelli
Murospora torifera Ybert
Vallatisporites ciliaris (Luber) Sullivan
Vallatisporites sp.
Monosaccate pollen grains
Cannanoropollis triangularis (Mehta) Bose and Maheshwari
Circumplicatipollis plicatus Ottone and Azcuy
Plicatipollenites malabarensis (Potonié and Sah) Foster

718 **REFERENCES**

719 Amos, A.J., 1954. Estructura de las formaciones paleozoicas de La Rinconada, pie oriental de la
720 Sierra Chica de Zonda (San Juan). Revista de la Asociación Geológica Argentina 9, 5–38.

721 Amos, A.J., Rolleri, E.O., 1965. El Carbónico marino en el Valle Calingasta-Uspallata (San
722 Juan-Mendoza). Bol.Inf. Petroleras, Buenos Aires, p.1-23.

723 Astini, R.A., Schmidt, C.J., Martinez, M., 1995. Compressional to extensional inversion in the
724 Carboniferous-Permian Paganzo Basin (Western Argentina) and the origin of the exhumed
725 glacial Namurian Paleovalleys of the Pampean Ranges. Geol. Soc. Am. Abstr. Programs A-408
726 p. New Orleans.

727 Aquino, C.D, Milana, J.P, Faccini, U.F., 2014. New glacial evidences at the Talacasto
728 Palaeovalley (Paganzo basin, W-Argentina) and its implications for the paleogeography of the
729 Gondwana margin. Journal of South American Earth Sciences 56, 278-300.

730 Archangelsky, A., 2000. Estudio sobre semillas neopaleozoicas de Argentina. Boletín Academia
731 Nacional Ciencias 64, 79-115.

732 Azcuy, C.L., di Pasquo, M., 2000. Palynology of the Late Carboniferous from the Tarija Basin,
733 Argentina: a systematic review of monosaccate pollen genera. Palaeöntographica Abt. B 253,
734 103-137.

735 Azcuy, C.L., Carrizo, H.A., Caminos, R., 2000. Carbonífero y Pérmico de las Sierras Pampeanas,
736 Famatina, Precordillera, Cordillera Frontal y bloque de San Rafael. In: Caminos R. (ed.)
737 Geología Argentina, Instituto de Geologia y Recursos Minerales, p. 261-318.

738 Azcuy, C., Beri, A., Bernardes-de-Oliveira, M.E.C., Carrizo, H.A., di Pasquo, M.M., Díaz
739 Saravia, P., González, C., Iannuzzi, R., Lemos, V., Melo, J.H.G., Pagani, A., Rohn, R.,
740 Rodríguez Amenábar, C., Sabattini, N., Souza, P.A., Taboada, A., Vergel, M.M., 2007.
741 Bioestratigrafía del Paleozoico Superior de América del Sur: primera etapa de trabajo hacia una

742 nueva propuesta cronoestratigráfica. Asociación Geológica Argentina, Serie D, Publicación
743 Especial 11, 9–65.

744 Arrondo, O., Césari, S., Gutierrez, P., 1991. *Frenguellia* a new genus of lycopods from the Early
745 Carboniferous of Argentina. Review of Palaeobotany and Palynology 70, 187-197.

746 Balseiro, D., Rustán, J.J., Ezpeleta, M., Vaccari, N.E., 2009. A new Serpukhovian
747 (Mississippian) fossil flora from western Argentina: paleoclimatic, paleobiogeographic, and
748 stratigraphic implications. Palaeogeography, Palaeoclimatology, Palaeoecology 280, 517-531.

749 Batten, D.J., 1996. Palynofacies. 26B-Palynofacies and petroleum potential. In: Jansonius, J.,
750 McGregor, D.C. (Eds.), Palynology: Principles and Applications. American Association
751 Stratigraphic and Palynologists Foundation 3, 1065–1084.

752 Beresi, M.S., Bordonaro, C.L., 1985. La Formación San Juan en la Quebrada de las Lajas, Sierra
753 Chica de Zonda, Provincia de San Juan. 9 Congreso Geológico Argentino (Buenos Aires),
754 Asociación Geológica Argentina, Actas 95–107.

755 Brea, M., Césari, S.N., 1995. An anatomically preserved stem from the Carboniferous of
756 Gondwana: *Phyllocladopitys petriellae* Brea and Césari, sp. nov. Review of Palaeobotany and
757 Palynology 86, 315-323.

758 Buatois, L.A., Mángano, M.G., 1995. Sedimentary dynamics and evolutionary history of a Late
759 Carboniferous lake in north-western Argentina. Sedimentology 42, 415–436.

760 Buatois, L.A., Limarino, C.O., Césari., S., 1994. Carboniferous lacustrine deposits from the
761 Paganzo basin,Argentinabasin, Argentina. In: Gierlowski-Kordesch, E., and Kelts, K. (Eds.),
762 Global Geological Record of Lake Basins 1, p. 135-140, Cambridge University Press.

763 Caputo, M.V., 1985. Late Devonian glaciation in South America. Palaeogeography,
764 Palaeoclimatology, Palaeoecology 51, 291–317.

765 Caputo, M.V., Crowell, J.C., 1985. Migration of glacial centers across Gondwana during
766 Paleozoic Era. Geological Society of America Bulletin 96, 1020–1036.

767 Césari, S.N., Bercowski, F., 1997. Palinología de la Formación Jejenes (Carbonífero) en la
768 quebrada de Las Lajas, provincia de San Juan, Argentina. Nuevas evidencias paleoambientales.
769 Ameghiniana 34, 497-509.

770 Césari, S.N., Gutierrez, P.R., 2001. Palynostratigraphy of Upper Paleozoic sequences in Central-
771 Western Argentina. Palynology 24, 113-146.

772 Césari, S.N., Gutierrez, P., Sabattini, N., Archangelsky, A., Azcuy, C.L., Carrizo, H.A., Cisterna,
773 G., Crisafulli, A., Cúneo, R.N., Díaz Saravia, P., Di Pasquo, M.R., González, C.R., Lech, R.,
774 Pagani, M.A., Sterren, A., Taboada, A.C., Vergel, M.M., 2007. Paleozoico Superior de
775 Argentina: un registro fosilífero integral para el Gondwana occidental. Publicación Especial
776 Asociación Paleontológica Argentina 11, 35–54..

777 Césari, S.N., Limarino, C.O., Gulbranson, E.L., 2011. An Upper Paleozoic bio
778 chronostratigraphic scheme for the western margin of Gondwana. Earth-Science Reviews 106,
779 149-160.

780 Cladera, G., Archangelsky, S., Vega, J.C., 2000. Precisiones geográficas, estratigráficas y
781 paleoambientales sobre los niveles portadores de cúpulas pteridospérmicas de la Formación
782 Jejenes, Carbonífero de San Juan, Argentina. Ameghiniana 37, 213-219.

783 Cohen, K.M., Finney, S., Gibbard, P.L., 2013. International Chronostratigraphic Chart v. 2013/1.
784 International Commission on Stratigraphy.

785 del Papa C., di Pasquo, M., 2007. Palaeoenvironmental and palaeoclimatic interpretation based
786 on lithofacial and palynological correlations of outcrop and subsurface sections of the Tarija
787 Formation (Upper Carboniferous), northwestern Argentina. Journal of South American Earth
788 Sciences 23, 99-119.

789 Díaz Martínez, E., Isaacson, P.E., 1994. Late Devonian glacially influenced marine
790 sedimentation in western Gondwana: The Cumana Formation, Altiplano, Bolivia. In: Embry,
791 A.F., Beauchamp, B., Glass, D.J. (eds.), Pangea: Global environments and resources: Calgary,
792 Canadian Society of Petroleum Geologists, Memoir 17, 511–522.

793 DiMichele, W.A., Cecil, C.B., Montañez, I.P., Falcon-Lang, H.J. 2010. Cyclic changes in
794 Pennsylvanian paleoclimate and effects on floristic dynamics in tropical Pangea. International
795 Journal of Coal Geology 83, 329–344

796 di Pasquo, M.M., 2002. The *Crassispora kosankei* - *Cystoptychus azcuyi* Palynozone from the
797 Upper Carboniferous Tupambi Formation, Tarija basin, northern Argentine. Review of
798 Palaeobotany and Palynology, Special Volume 118, 47-75.

799 di Pasquo, M., 2003. Avances sobre palinología, bioestratigrafía y correlación de los Grupos
800 Macharetí y Mandiyutí, Neopaleozoico de la cuenca Tarija, provincia de Salta, Argentina.
801 Ameghiniana 40, 3–32.

802 Di Pasquo, M.M., 2007. Update and importance of the Carboniferous and Permian paleontological records
803 of the Tarija Basin. In: E. Díaz-Martínez, I. Rábano (eds.), 4° European Meeting on Paleontology and
804 Stratigraphy of Latin American. Instituto Geológivo y Minero de España, Serie Cuadernos Geominero.
805 No. 8. 107-112.

806 di Pasquo, M.M., 2009. The Pennsylvannian palynoflora from the Pando X-1 Borehole, northern
807 Bolivia. Review of Palaeobotany and Palynology 157, 266–284.

808 di Pasquo, M.M., Silvestri, L., 2014. Las colecciones de Palinología y Paleobotánica del
809 Laboratorio de Paleopalinología y Paleobotánica del Centro de Investigaciones Científicas y
810 Transferencia de Tecnología a la Producción (CICYTTP), Entre Ríos, Argentina. Contribuição à
811 RESCEPP “Rede Sul-americana de Coleções e Ensino em Paleobotânica e Palinologia”, Boletín
812 de la Asociación Latinoamericana de Paleobotánica y Palinología 14, 39-47.

Dykstra, M., Kneller, B., Milana, J.P., 2006. Deglacial and postglacial sedimentary architecture in a deeply incised paleovalley; the Pennsylvanian (late Carboniferous) Jejenes Formation, San Juan, Argentina. Geological Society of America Bulletin 118, 913-937.

Dykstra, M., Kneller, B., Milana, J.P., 2011. Bed-thickness and grain-size trends in a small-scale proglacial channel–levee system, the Carboniferous Jejenes Formation, Western Argentina: implications for turbidity current flow processes. Sedimentology 59, 605-622.

Du Toit, A.L., 1927. A geological comparison of South America with South Africa, with a palaeontological contribution of F. R. Cowper Reed. Carnegie Institute, Publ., Washington, 381, 1-157.

Enkelmann, E, Kenneth, D., Ridgway, Carignano, C., Linnemann, U., 2014. A thermochronometric view into an ancient landscape: Tectonic setting, development, and inversion of the Paleozoic eastern Paganzo basin, Argentina. Lithosphere 6, 93-107.

Frakes, L.A., Francis, J.E., Syktus, J.I., 1992. Climate modes of the Phanerozoic. The History of the Earth's Climate over the Past 600 Million Years. Cambridge University Press.

França, A.B., Winter, W.R., Assine, M.L., 1996. Arenitos Lapa- Vila Velha: um modelo de trato de sistemas subaquosos canal-lobos sob influência glacial, Grupo Itararé (C-P), Bacia do Paraná. Revista Brasileira de Geociencias 26, 43–56.

Fielding, C.R., Frank, T.D., Birgenheier, L.P., Rygel, M.C., Jones, A.T., Roberts, J., 2008. Stratigraphic record and facies associations of the late Paleozoic ice age in Eastern Australia (New South Wales and Queensland). In: Fielding, C.R., Frank, T.D., and Isbell, J.L. (Eds.), Resolving the Late Paleozoic Ice Age in Time and Space, Geological Society of America Special Paper 441, 41-57.

González Amicón, O., 1973. Microflora carbónica de la localidad Retamito, Provincia de San Juan, Ameghiniana 10, 1-35.

837 Gonzalez, B.G., 1975. Acerca de la existencia de la Protoprecordillera de Cuyo. in Actas. VI
838 Congreso Geologico Argentino, Bahia Blanca. 1, 101-107.

839 González, C.R., 1981. Pavimento glaciario en el Carbónico de La Precordillera. Revista de la
840 Asociación Geológica Argentina 36, 262-266.

841 González, C.R., 1990. Development of the Late Paleozoic glaciations of the South American
842 Gondwana in western Argentina. Palaeogeography, Palaeoclimatology, Palaeoecology 79, 275-
843 287.

844 Gutiérrez, P.R., Césari, S.N., 1987. Nuevos elementos microflorísticos de la Formación Jejenes
845 (Carbónico) provincia de San Juan. Asociación Geológica Argentina, Serie A, Monografías y
846 Reuniones 2, 168-173.

847 Gutiérrez, P.R., Arrondo, O.G., 1994. Revisión de las licopsidas de la Argentina. 1.
848 *Archaeosigillaria* Kidston y *Frenguellia* Arrondo, Césari y Gutiérrez. Ameghiniana, 31, 381-
849 393.

850 Gutiérrez, P.R., Pazos, P., 1994. Acerca de la presencia de semillas platispérmicas en la
851 Formación Guandacol (Carbonífero), Argentina. Ameghiniana 31, 375–377.

852 Gutiérrez, P.R., Ganuza, D.G., Morel, E., Arrondo, O.G., 1992. Los géneros *Cordaicarpus* Arber
853 y *Samaropsis* Goeppert (semillas platispérmicas) en el Neopaleozoico argentino. Ameghiniana
854 29, 49-68.

855 Gutiérrez, P.R., Césari, S.N., Martínez, M., 1995. Presencia de Nothorhacopteris argentinica
856 (Geinitz) Archangelsky en Formación Guandacol (Carbonífero), Argentina. Ameghiniana 32,
857 169–172.

858 Gulbranson, E., Limarino, C.O., Marenssi, S., Montañez, I., Tabor, N., Davydov, V., Colombi,
859 C., 2008. Glacial deposits in the Río del Peñón Formation (Late Carboniferous), Río Blanco

Basin, Northwestern Argentina. Latin American Journal of Sedimentology and Basin Analysis 15, 37-42.

Gulbranson, E.L., Montañez, I.P., Schmitz, M.D., Limarino, C.O., Isbell, J.L., Marenssi, S.A., and Crowley, J.L., 2010. High-precision U-Pb calibration of Carboniferous glaciation and climate history, Paganzo Group, NW Argentina. Geological Society of America Bulletin 122, 1480-1498.

Henry, L.C., Isbell, J.L., Limarino, C.O., 2008. Carboniferous glacigenic deposits of the Protoprecordillera of west central Argentina. In: Fielding, C.R., Frank, T.D., and Isbell, J.L. (Eds.), Resolving the Late Paleozoic Ice Age in Time and Space, Geological Society of America Special Paper 441, p. 131-142.

Henry, L.C., Isbell, J.L., Limarino, C.O., McHenry, L.J., Fraiser, M.L., 2010. Mid-Carboniferous deglaciation of the Protoprecordillera, Argentina recorded in the Agua de Jagüel palaeovalley. Palaeogeography, Palaeoclimatology, Palaeoecology 298, 112–129.

Isaacson, P.E., di Pasquo, M., Grader, G., Anderson, H., 2014. Late Paleozoic carbonates and coeval glacial deposits in Bolivia: correlations across a significant paleoclimatic gradient. AAPG/SEPM Hedberg Research Conference “Latitudinal Controls on Stratigraphic Models and Sedimentary Concepts” (28/10-01/10-2014, Banff, Alberta, Canada).

Isbell, J.L., Miller, M.F., Wolfe, K.L., Lenaker, P.A., 2003. Timing of late Paleozoic glaciation in Gondwana: was glaciation responsible for the development of northern hemisphere cyclothems? In: Chan, M.A., Archer, A.W. (Eds.), Extreme Depositional Environments: mega end members in geologic time. Geological Society of America Special Paper 370, 5-24.

Isbell, J.L., Henry, L.C., Gulbranson, E.L., Limarino, C.O., Fraiser, M.L., et al. 2012. Glacial paradoxes during the late Paleozoic ice age: evaluating the equilibrium line altitude as a control on glaciation. Gondwana Research 22, 1–19.

884 Jordan, T.E., Allmendinger, R.W., Damanti, J.F., 1993. Chronology of motion in a complete
885 thrust belt: the Precordillera, 30-31°S, Andes Mountains. Journal of Geology, 101: 135-136.

886 Kneller, B., Milana, J.P., Buckee, C., Al Ja'aidi, O.S., 2004. A depositional record of deglaciation
887 in a Palaeovalley (Late Carboniferous [Pennsylvanian] of San Juan Province, Argentina): the role
888 of catastrophic sedimentation. Geological Society of America Bulletin 116, 348–367.

889 Lech, R.R., Milana, J.P., 2006. Nuevos registros de moluscos carboníferos en la Sierra del
890 Tontal, Precordillera de San Juan. Revista Asociación Geológica Argentina 61, 57-62.

891 Lech, R.R.., Milana, J.P, Banchig, A.L., 1998. Braquiópodos carboníferos de la Sierra del Tontal,
892 Provincia de San Juan, Argentina. Ameghiniana, 35, 405-413.

893 Lech, R.R., Milana, J.P., Bercowski, F.,1990. Nueva Asociación de braquiópodos fósiles en el
894 Carbonífero superior de la Precordillera Central, San Juan, Argentina. 5º Congreso Argentino de
895 Paleont. y Biostratig., Tucumán, II: p.89-96.

896 Leguizamón, R., Vega, J.C., 1990. El género *Triphyllopteris* (morfogénero de frondes) en el
897 Carbonífero de la República Argentina. Ameghiniana 27, 305-309.

898 Limarino, C.O., Gutierrez, P.R., 1990. Diamictites in the Agua Colorada Formation
899 (northwestern Argentina): New evidence of Carboniferous glaciation in South America. Journal
900 of South American Earth Sciences 3, 9-20.

901 Limarino, C.O., Spalletti, L.A., 2006. Paleogeography of the upper Paleozoic basins of southern
902 South America: An overview. Journal of South American Earth Sciences 22, 134-155.

903 Limarino, C.O., Césari, S.N., Net, L.I., Marenssi, S.A., Gutierrez, R.P., Tripaldi, A., 2002. The
904 Upper Carboniferous postglacial transgression in the Paganzo and Río Blanco basins
905 (northwestern Argentina): facies and stratigraphic significance. Journal of South American Earth
906 Sciences 15, 445-460.

907 Limarino, C.O., Tripaldi, A., Marenssi, S.A., Fauqué, L., 2006. Tectonic, sea level, and climatic
908 controls on late Paleozoic sedimentation in the western basins of Argentina. Journal of South
909 American Earth Sciences 33, 205-226.

910 Limarino, C.O., Alonso-Muruaga P.J., Ciccioli P.L., Perez Loinaze V.S., Césari S.N., 2014.
911 Stratigraphy and palynology of a late Paleozoic glacial paleovalley in the Andean Precordillera,
912 Argentina. Palaeogeography, Palaeoclimatology, Palaeoecology 412, 223-240.

913 López-Gamundí, O.R., 1983. Modelo de sedimentación glacimarina para la Formación Hoyada
914 Verde, Paleozoico superior de la Provincia de San Juan. Revista Asociación Geológica
915 Argentina, 38, p. 60-72.

916 López-Gamundí, O.R., 1987. Depositional models for the glaciomarine sequences of Andean late
917 Paleozoic basins of Argentina. Sedimentary Geology 52, 109–126.

918 López Gamundí, O.R., 1989. Postglacial transgressions in late Paleozoic basins of western
919 Argentina: a record of glacioeustatic sea level rise. Palaeogeography, Palaeoclimatology,
920 Palaeoecolgy 71, 257–270.

921 López-Gamundí, O.R., Martinez, M., 2000. Evidence of glacial abrasion in the Calingasta-
922 Uspallata and western Paganzo Basins, mid-Carboniferous of western Argentina.
923 Palaeogeography, Palaeoclimatology, Palaeoecology 159, 145-165.

924 López Gamundí, O.R., Limarino, C.O., Césari, S.N., 1992. Late Paleozoic paleoclimatology of
925 central west Argentina. Palaeogeography, Palaeoclimatology, Palaeoecology 91, 305–329.

926 Marenssi, S.A., Tripaldi, A., Limarino, C.O., Caselli, A.T., 2005. Facies and architecture of a
927 Carboniferous grounding-line system from the Guandacol Formation, Paganzo Basin,
928 northwestern Argentina. Gondwana Research 8, 87-202.

929 Milana, J.P., 1988. Sedimentación estuárica Carbonífera tardía en la Precordillera Central, San
930 Juan, Argentina. 2 Reunión Argentina de Sedimentología (Buenos Aires). Actas, p. 185-188.

931 Milana, J.P. and Bercowski, F.1987a. Nueva localidad marina para el Neopaleozoico de
932 Precordillera, en la confluencia de los ríos Uruguay y San Juan, Argentina. 4ª Reun. Internac.
933 Work.Group PICG-211 (IUGS-UNESCO), Santa Cruz de la Sierra, Bolivia, Abstracts, p.56-59.

934 Milana,J.P., Berscowski, F., 1987b. Rasgos erosivos y depositacionales glaciales en el
935 Neopaleozoico de la Precordillera Central, San Juan, Argentina. 4a Reun. Internac. Work. Group
936 PICG-211 (IUGS-UNESCO), Santa Cruz de la Sierra, Bolivia, Abstracts, p. 46-48.

937 Milana, J.P., Bercowski, F., 1990. Facies y geometría de depósitos glaciales en un paleovalle
938 Carbonífero de Precordillera Central, San Juan, Argentina. 3 Reunión Argentina de
939 Sedimentología (San Juan). Actas, p. 199–204.

940 Milana, J.P., Bercowski, F., 1993. Late Palaeozoic Glaciation in Paganzo Basin, Western
941 Argentina: Sedimentological Evidence. Comptes Rendus XII ICC-P, Bs. As, v.1, 325-335.

942 Milana, J.P., Banchig. L.A., 1997. Nuevo ordenamiento del Grupo San Eduardo (Carbonífero) en
943 la sierra de Barreal, San Juan, y reinterpretación de su ambiente de depositación. II Jornadas de
944 Geología de Precordillera, San Juan, p. 110-115.

945 Milana, J.P., Bercowski, F., Lech, R.R., 1987. Análisis de una secuencia marino-continental
946 Neopaleozoica enla región del río San Juan, Precordillera Central, San Juan, Xº Cong. Geol.
947 Argentino, Tucumán, Actas III, p.113-116.

948 Milana, J.P., di Pasquo, M.M., Valdez, V., 2014. Nuevos datos sobre el límite Carbonífero -
949 Pérmico en la sección Río del Peñón, precordillera riojana. 14 Reunión Argentina de
950 Sedimentología (Puerto Madryn). Extended Abstract.

951 Mozer, A., 2010. Authigenic pyrite framboids in sedimentary facies of the Mount Wawel
952 Formation (Eocene), King George Island, West Antarctica. Polish Polar Research 31, 255–272.

953 Pazos, P.J., 2002. The late Carboniferous glacial to postglacial transition: facies and sequence
954 stratigraphy, western Paganzo Basin, Argentina. Gondwana Research 5, 467-487.

955 Pazos, P.J., di Pasquo, M.M., Amenábar, R.C., 2007. Ichnology of the glacial to post-glacial
956 transition in the El Imperial Formation (Upper Carboniferous), San Rafael basin, Argentina.
957 SEPM Special Publication No. 88 Sediment-Organism Interactions: a multifaceted Ichnology
958 137, 147.

959 Peralta, S.H., 1990. The Silurian of the San Juan Precordillera. In: Bordonaro, O. (ed.), Relatorio
960 de Geología y recursos naturales de la Provincia de San Juan, Asociación Geológica Argentina,
961 p. 48–64. Buenos Aires.

962 Peralta, S.H., Baldis, B.A., Cecione, A., 1994. Rinconada Formation, eastern Precordillera of San
963 Juan, Argentina: Sedimentary mélange (olistostromes) or tectonics?. 7 Congreso Geológico
964 Chileno (Antofagasta), Universidad del Norte. Actas 1, 129–133.

965 Pérez Loinaze, V.S., Césari, S.N., 2012. Palynology of late Serpukhovian glacial and postglacial
966 deposits from Paganzo Basin, northwestern Argentina. Micropaleontology 58, 335–350.

967 Pujana, R.R., 2005. Gymnospermous woods from Jejenes Formation, Carboniferous of San Juan,
968 Argentina: *Abietopitys petriellae* (Brea and Césari) nov. comb. Ameghiniana 42, 725-731.

969 Raymond, A., Lambert, L., Costanza, S., Slone, E.J., Cutlip, P.C., 2009. Cordaiteans in
970 paleotropical wetlands: An ecological re-evaluation. International Journal of Coal Geology 83,
971 248–265.

972 Rolleri, E.O., Baldis, B.A.J., 1969. Paleogeography and distribution of Carboniferous deposits in
973 the Argentine Precordillera. Coloquio de la IUGS: Gondwana Stratigraphy, Earth Sciences,
974 UNESCO, (2), p.1005-1024.

975 Safity, J.A., Gorustovich, S., 1983. Paleogeografía de la Cuenca del Grupo Paganzo (Paleozoico
976 Superior). Revista Asociación Geológica Argentina 38,437-453.

977 Sato, K., Tassinari, C.C., Basei, M.A., Junior, O.S., Onoe, A.T, Dias, Souza, M., 2014. Sensitive
978 High Resolution Ion Microprobe (SHRIMP IIe/MC) of the Institute of Geosciences of the
979 University of São Paulo, Brazil: analytical method and first results. Geology USP 14, 3.

980 Schatz, E.R., Mángano, M.G., Buatois, L.A., Limarino, C.O., 2011. Life in the late Paleozoic ice
981 age: trace fossils from glacially influenced deposits in a late Carboniferous fjord of western
982 Argentina. Journal of Paleontology 85, 502-518.

983 Schulz, A., Santiago, M., Hernández, R., Galli, C., Alvarez, L., Del Papa, C., 1999. Modelo
984 estratigráfico del Carbónico en el sector sur de la Cuenca de Tarija. 4 Congreso de Exploración y
985 Desarrollo de Hidrocarburos (Mar del Plata), Actas, 695-704.

986 Sievers, H., 2008. Temperature and salinity in the austral Chilean channels and fjords. *Progress*
987 *in the oceanographic knowledge of Chilean interior waters, from Puerto Montt to Cape Horn.*
988 *Comité Oceanográfico Nacional-Pontificia Universidad Católica de Valparaíso, Valparaíso,*
989 pp.31-36.

990 Silva, N. and Vargas, C.A., 2014. Hypoxia in Chilean patagonian fjords. *Progress in*
991 *Oceanography*, *129*, pp.62-74.

992 Starck, D., del Papa, C., 2006. The northwestern Argentina Tarija Basin: stratigraphy,
993 depositional systems, and controlling factors in a glaciated basin. Journal of South American
994 Earth Sciences 22, 169-184.

995 Starck, D., Gallardo, E., Schulz, A., 1993. Neopaleozoic stratigraphy of the Sierras Subandinas
996 occidentales and Cordillera Oriental, Argentina. 12 Cong. Stratigr. Géol. Carbonif. Permien,
997 Actas 2, 353–372.

998 Suárez-Soruco, R., 2000. Compendio de geología de Bolivia. Rev. Téc. Y.P.F.B., 18, p. 214.

999 Tyson, R.V., 1995. Sedimentary organic matter. Organic facies and palynofacies. Chapman &
1000 Hall. Ed. 615 pp, Oxford.

1001 Utting, J., Wielens, H., 1992. Organic petrology, thermal maturity, geology, and petroleum
1002 source rock potential of Lower Permian coal, Karoo Supersystem, Zambia. Energy Sources 14,
1003 337-354.

1004 Valdez, V., Paim, P.S., Souza, P., di Pasquo, M.M., 2013. Carboniferous deglacial record in
1005 Paraná Basin (Brazil) and its analog in Paganzo Basin (Argentina): a comparison between
1006 Pennsylvanian and Permian sections. 6th Latin American Congress of Sedimentology, São Paulo,
1007 Brazil. Abstract.

1008 Valdez, V., di Pasquo, M.M., Milana J.P., Kneller, B., Paim P.S., 2014. Palynoassemblages in
1009 the Sierra de Maz area, La Rioja Province, Argentina: an older age for the base of the Guandacol
1010 Formation. XIV Reunión Argentina de Sedimentología (Puerto Madryn). Extended Abstract,
1011 227-278

1012 Valdez B.V., Milana, J.P., Kneller, B., 2015. Megadeslizamientos gravitacionales de la
1013 Formación Guandacol en Cerro Bola y Sierra de Maz y su relación con la glaciación del
1014 Paleozoico Tardío, La Rioja, Argentina. Latin American Journal of Sedimentology and Basin
1015 Analysis. 22, 109-133.

1016 Veevers, J.J, Powell, C.M., 1987. Late Paleozoic glacial episodes in Gondwanaland reflected in
1017 transgressive- regressive depositional sequences in Euramerica. Geological Society of American
1018 Bulletin 98, 475–87.

1019 Vega, J.C., 1995. La flora fósil de la Formación Jejenes (Carbonífero). Implicancias
1020 paleoclimáticas y paleogeográficas. Ameghiniana 32, 31-40.

1021 Vergel, M.M., Cisterna, G.A., Sterren, A.F., 2015. New palynological records from the
1022 glaciomarine deposits of the El Paso Formation (late Serpukhovian-Bashkirian) in the Argentine
1023 Precordillera: biostratigraphical implications. Ameghiniana 52, 613–624.

1024

1025 **Captions**

1026 Fig. 1. Late Carboniferous palaeogeography of the Paganzo and adjacent basins, modified from
1027 Salfity and Gorustovich (1983) and Aquino et al. (2014). A) Upper Palaeozoic basins of South
1028 America (A: Paganzo, B: Uspallata/Iglesia, C: San Rafael, D: Tepuel Genoa, E: Arizaro, F:
1029 Chaco, G: Paraná, H: Tarija, I: Chaco- Paraná. B) Location of the studied outcrops. C). Black
1030 stars are glacial localities, as follows: (1) Talacasto Palaeovalley (Aquino et al., 2014) (2)
1031 Malanzán Paleovalley (Enkelman et al., 2014); (3) Río del Peñón (Gulbranson et al., 2010); (4)
1032 Huaco section; (5) Río Francia (Milana and López, 1998); (6) Quebrada Las Lajas (Dykstra et
1033 al., 2006); (7) Quebrada Grande (Kneller et al., 2004, this work). (8) Hoyada Verde (Milana and
1034 Banchig, 1997); (9) Tontal (Lech and Milana, 2006); (10) Km 63 (Lech et al., 1990); (11)
1035 Malimán section Limarino et al. (2002); (12) The Cerro Bola and (13) Guandacol hills
1036 depocenters (Dykstra et al., 2011, Valdez et al., 2013). The (14) correspond to Maradonas
1037 subbasin.

1038 Fig. 2. Geologic map of Quebrada Grande (modified from Kneller et al., 2004).

1039 Fig. 3. Quebrada Grande palaeovalley. (A) Oblique aerial photo showing the dimensions of the
1040 palaeovalley. (B) Photomosaic of the unconformity and the palaeovalley fill. Stages III and IV at
1041 the main valley.

1042 Fig. 4. Correlation of the Paganzo basin with other South American basins. 1 Paganzo (Balseiro
1043 et al., 2009; Césari et al., 2011; Pérez Loinaze and Césari, 2012, Valdez et al., 2014). 2
1044 Uspallata-Iglesia (Azcuy et al., 2007; Césari et al., 2011; Milana et al., 2014). 3 San Rafael
1045 (Césari and Gutierrez, 2001). 4 Tarija (di Pasquo, 2002, 2007, 2009). 5 Paraná Basin (Souza,
1046 2003; Iannuzzi, 2013). Black stars represent the isotopic ages for: 1. Cortaderas (335.99 ± 0.06
1047 Ma); 2. Guandacol (318.79 ±0.10 Ma); 3. Río del Peñón (319.57 ±0.09 Ma); 4. Tupe (315.46
1048 ±0.07 Ma); and 5. Patquía (310.71 ± 0.11 Ma) formations, according to Gulbranson et al. (2010).

1049 The red star represents the first isotopic age for the Jejenes Formation (321.3 ±5.3 Ma) presented
1050 in this work.

1051 Fig. 5. Fence diagram of the palaeovalley fill showing the thickness changes. Productive samples
1052 for palynology and palaeobotany remains are located in the section. Modified from Kneller et al.
1053 (2004).

1054 Fig. 6. Composite stratigraphic log of the stages that yielded paleontological and isotopic data.

1055 Fig. 7. Quantitative distribution of kerogen (palynomorphs, phytodebris and AOM).

1056 Fig. 8. Detailed log of Stage V showing the different facies association.

1057 Fig. 9. Boulders of the base of Stage V. (A). Note the polished aspect of the metamorphic
1058 boulder surface. Seated person for scale. (B). Another schist boulder resting on the top of Stage
1059 IV. (C). Some possibly striations in the lower part of the metamorphic boulder of figure A. (D).
1060 Imbricated metamorphic megaclast on top of Stage IV.

1061 Fig. 10. Dropstones of upper Stage V. (A). Outsized granite dropstone. (B). Small limestone
1062 dropstone. (C and D). Small metamorphic rock dropstones.

1063 Fig. 11. Tuffite thin section. Notice the presence of bubble wall shards in yellow, crystal
1064 fragments in blue and glass in green.

1065 Fig. 12. Cathodoluminescence images of analyzed zircon grains from the Quebrada Grande
1066 Tuffite (spot size 24 μm).

1067 Fig. 13. U-Pb sensitive high-resolution ion microprobe (SHRIMP) zircon weighted average
1068 diagram of sample Quebrada Grande Tuffite (see location in Fig. 6) that occur within the
1069 mudstone interval of Stage III (Jejenes Formation) of the Paganzo basin. MSWD—mean square
1070 of weighted deviation.

1071 Fig. 14. Flora and palynoflora from the Bashkirian Jejenes Formation at Quebrada Grande.

1072 (A). Lycophyte stem, CICYTTP-Pb 64. Outcrop of Log 4, tuffite level. Scale bar 1cm.

(B). *Cordaicarpus cesariae* Gutiérrez et al., CICYTTP-Pb 55. Outcrop of Log 4, tuffite level. Scale bar 2 mm.

(C, D). *Cordaicarpus famatinensis* Gutiérrez et al., (C) CICYTTP-Pb 52, (D) CICYTTP-Pb 53. Outcrop of Log 4, tuffite level. Scale bar 2 mm.

(E-F). *Cristatisporites stellatus* (Azcuy) Gutiérrez and Limarino, (E) CICYTTP-Pl 1056-2-HF2 J34/3, (F) CICYTTP-Pl 1055-2-HF F46/0.

(G). *Cristatisporites inordinatus* (Menéndez and Azcuy) Playford, CICYTTP-Pl 1053-1-HF K54.

(H). *Cristatisporites inconstans* Archangelsky and Gamerro, CICYTTP-Pl 1055-2-Ox U34/0.

(I). *Cristatisporites rollerii* Ottone, CICYTTP-Pl 1062-2-HF2 G29.

(J). *Cristatisporites spinosus* (Menéndez and Azcuy) Playford emend. Césari, CICYTTP-Pl 1056-1-HF2 X48/0.

(K). *Vallatisporites* sp., CICYTTP-Pl 1055-3-Ox E25/0.

(L). *Lundbladispora braziliensis* (Pant, Srivastava) Marques Toigo, Pons emend. M. Toigo and Picarelli, CICYTTP-Pl 1062-1-HF2 N48/1.

(M). *Plicatipollenites malabarensis* (Potonié and Sah) Foster, CICYTTP-Pl 1062-2-HF2 N51.

(N). *Circumplicatipollis plicatus* Ottone and Azcuy, CICYTTP-Pl 1056-1-HF-paraf P51/1.

(Ñ). *Murospora torifera* Ybert, CICYTTP-Pl 1056-2-HF2 U30/2.

(O). *Convolutispora muriornata* Azcuy, CICYTTP-Pl 1056-2-HF2 P38/2.

Figs. E-L and Ñ-O Scale bar 15 µm, Figs. M-N Scale bar 35 µm.

Fig. 15. Deposits with paleobotanical remains. (A). Muddy section of upper stage III. (B). Small wood fragment found in Stage III. (C). Crystal-rich tuffite level. (D). Plant stems preserved in the tuffite level. (E). Sandy turbidites of upper Stage IV. (F). Plants stems in the sandstone beds of the turbidites section.

Fig. 16. Palynoflora from the Bashkirian Jejenes Formation at Quebrada Grande.

(A). Palynomorph with framboidal pyrite, CICYTTP-Pl 1051-1-HF T37/2. Scale bar 20 µm.

1098 (B). *Cristatisporites* sp., CICYTTP-Pl 1062-1-HF2 U44/2, showing effects of pyritization. Scale
1099 bar 20 µm.
1100 (C). Monosaccate pollen grain (pyritized), CICYTTP-Pl 1055-2-Ox K34/0. Scale bar 20 µm.
1101 (D). Monosaccate pollen grain (pyritized), CICYTTP-Pl 1049-2-HF2 L37/0. Scale bar 35 µm.
1102 (E). Monosaccate pollen grain (pyritized), CICYTTP-Pl 1055-2-Ox Q49/0. Scale bar 30 µm.
1103 (F). Monosaccate pollen grain (pyritized), CICYTTP-Pl 1055-2-Ox R37/4. Scale bar 35 µm.
1104 (G). Palynofacies, CICYTTP-Pl 1053-1-HF Q53/2.
1105 (H). Palynofacies, CICYTTP-Pl 1062-1-HF2 Q36/1. Traqueids and other components are shown.
1106 (I). Traqueid (fragmented), CICYTTP-Pl 1053-1-HF K36/3.
1107 (J). Detail of traqueid in Fig. H of gymnospermous affinity (260 µm in length).
1108 Fig. 17. Depositional model for QG palaovalley. (A). Stage I: glacial advance and minor
1109 sedimentation occurs as lodgement tills. (B). Stage II marks the beginning of glacial retreat and
1110 resulting gradual flooding of the valley. (C). Stage III records an acceleration of the ice melting
1111 and resulting expressive marine flooding. (D).The transition from lower to upper Stage III
1112 indicates a continue sea-level rise associated with glacier retreat. The maximum flooding
1113 interval occurs between the dropstone-free mudstones of upper Stage III and the sandy turbidites
1114 without dropstones of the base of Stage IV (E). (F). Stage V registers the development of fjord-
1115 head deltas and fan deltas formed after a glacial-induced sea level fall, when sea-level rise was
1116 surpassed by the deglacial sedimentary input.
1117

1118 **Table Captions**

1119 Table 1. Characterization of palynofacies of the productive levels in Quebrada Grande.
1120 Explanation of the used categories: phytoclasts (traqueids, cuticles), opaques (non-structured
1121 brown and black debris), Amorphous Organic Matter (AOM), and palynomorphs (spores and
1122 pollen grains). Size: small (S <50 µm), medium (M), large (L >200 µm), variable (V), Shape:
1123 bladeshaped (B), equidimensional (E), angular (A), Sorting: poor (P), moderate (M), well (W),

1124 Pyrite (euhedral-E, framboidal-F): low (L), moderate (M), high (H), Preservation: complete (C),

1125 fragmented (F), corroded (Co), TAI (Thermal alteration index, after Utting and Wielens, 1992).

1126

1127 Table 2. Summary of SHRIMP U-Pb zircon data for Quebrada Grande tuffite.

1128

TABLES

Lab. No.	AOM	Palynom.	Phy+Op	TS	MPG	Brown clasts	Black clasts	Traqueids	Cuticles	Preservation	Size	Shape	Sorting	Pyrite	TAI
1049	10	2	88	1.5	0.5	35	35	10	8	F	V	E, B	P		3 to +3
1054		3	97	3	0	20	50	15	12	F, C	V	E, B	P		3 to +3
1053		1	99	1	0	20	40	30	9	F, C	V	A, B	P		4
1052			100	0	0	50	50	0	0	F	S	B, A	W		4
1051		10	90	8	2	10	30	30	20	F	M, S	B, A	M	(F, E) M	4 to +3
1055	10	20	70	15	5	25	20	20	5	F, C	S, M	A, B	M	(F, E) L	4 to +3
1062		20	80	15	5	25	20	30	5	F, C	V	B, A	P	(F, E) L	3 to +3
1061		1	99	1	0	30	30	30	9	F	V (S)	B, A	M		4
1060			100	0	0	40	20	30	10	F	S (L)	B, A	M		
1059			100	0	0	30	20	45	5	F	V	B, A	P		
1058			100	0	0	20	40	40	0		L	B	W		
1057	10		90	0	0	50	30	8	2		V	V	P		4
1056	10	13	77	10	3	25	20	30	2	F	S	B(dom), A	W		3 to +3

Table 1

Spot Name	% $206Pb_c$	ppm U	ppm Th	232Th /238U	ppm Rad 206Pb	207* /206*	% err	207* /235	% err	206* /238	% err	err corr	204corr 206Pb /238U Age	1s err
QG-1.1	1.86	505	430	0.88	24.4	0.05397	8.85	0.411	9.24	0.0553	2.49	0.27	347	8.4
QG-2.1	2.38	325	200	0.64	15.3	0.05148	10.52	0.379	10.90	0.0534	2.6	0.24	335	8.5
QG-3.1	3.43	535	286	0.55	23.9	0.05234	14.81	0.361	15.18	0.0501	2.86	0.19	315	8.8
QG-4.1	1.39	744	388	0.54	33.5	0.05295	5.16	0.377	5.72	0.0517	2.38	0.42	325	7.6
QG-5.1	5.02	684	513	0.78	32.4	0.05407	14.04	0.389	14.43	0.0523	2.46	0.17	328	7.9
QG-5.2	0.66	208	146	0.72	9.3	0.05346	5.16	0.381	5.74	0.0516	2.5	0.43	325	7.9
QG-6.1	0.43	289	228	0.81	12.5	0.05309	4.87	0.368	5.45	0.0503	2.45	0.45	316	7.5
QG-7.1	0.77	1023	1735	1.75	43.9	0.05386	6.90	0.368	7.30	0.0495	2.38	0.33	312	7.2
QG-8.1	0.05	503	108	0.22	80.5	0.07508	0.80	1.927	2.50	0.1862	2.36	0.95	1101	23.9
QG-9.1	0.35	575	19	0.03	91.1	0.07661	1.26	1.942	2.69	0.1839	2.36	0.88	1088	23.7
QG-10.1	0.56	232	198	0.88	10.2	0.0525	4.38	0.37	5.04	0.0512	2.47	0.49	322	7.8
QG-11.1	0.12	178	82	0.48	31.4	0.08011	1.87	2.269	3.45	0.2054	2.9	0.84	1204	31.9
QG-12.1	1.30	452	234	0.54	20.6	0.05398	5.99	0.389	6.48	0.0523	2.42	0.37	328	7.7

Errors are 1-sigma; Pb_c and Pb^* indicate the common and radiogenic portions, respectively.
(1) Common Pb corrected using measured ^{204}Pb.

Table 2

FIGURES

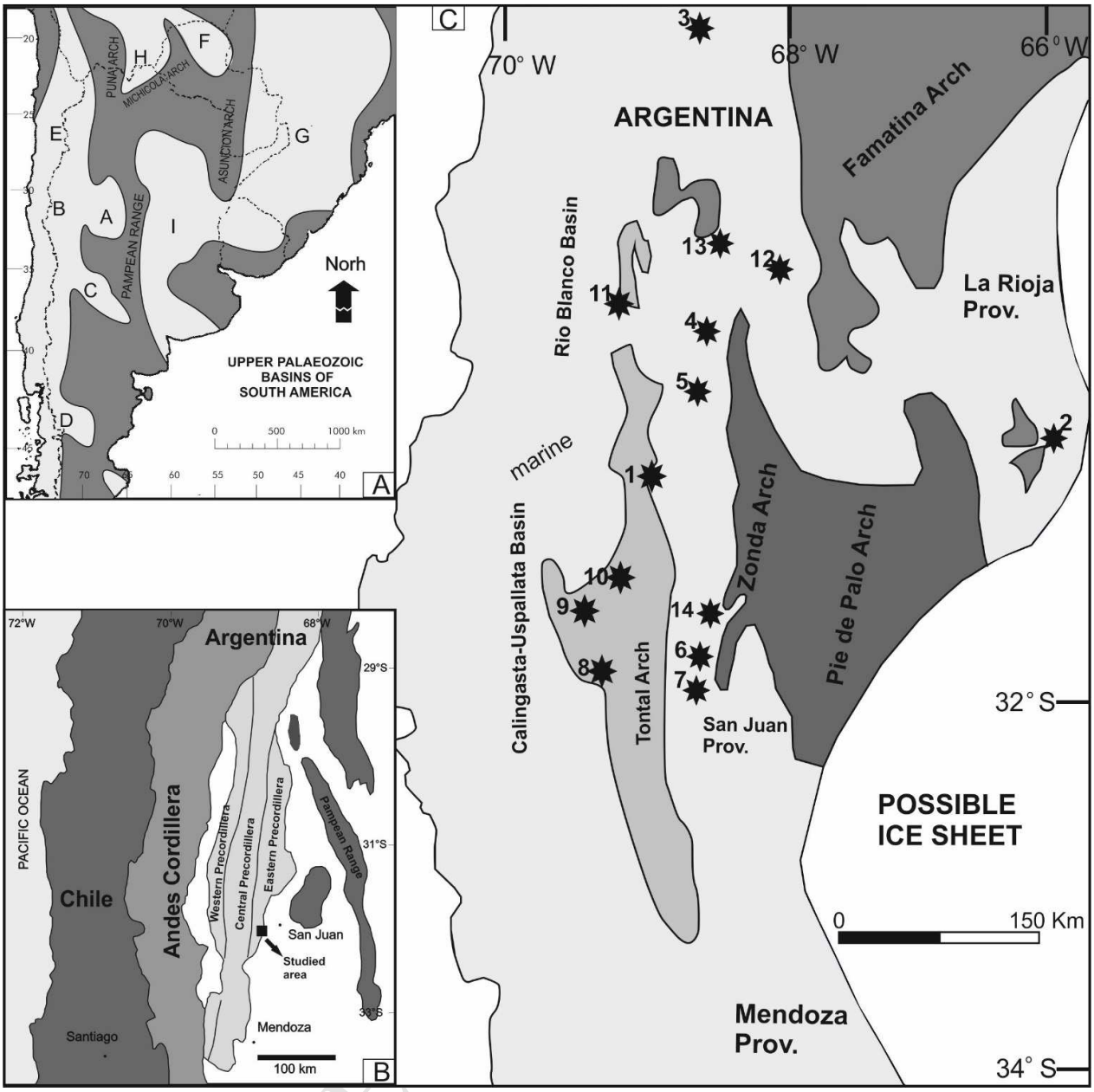

Figure 1

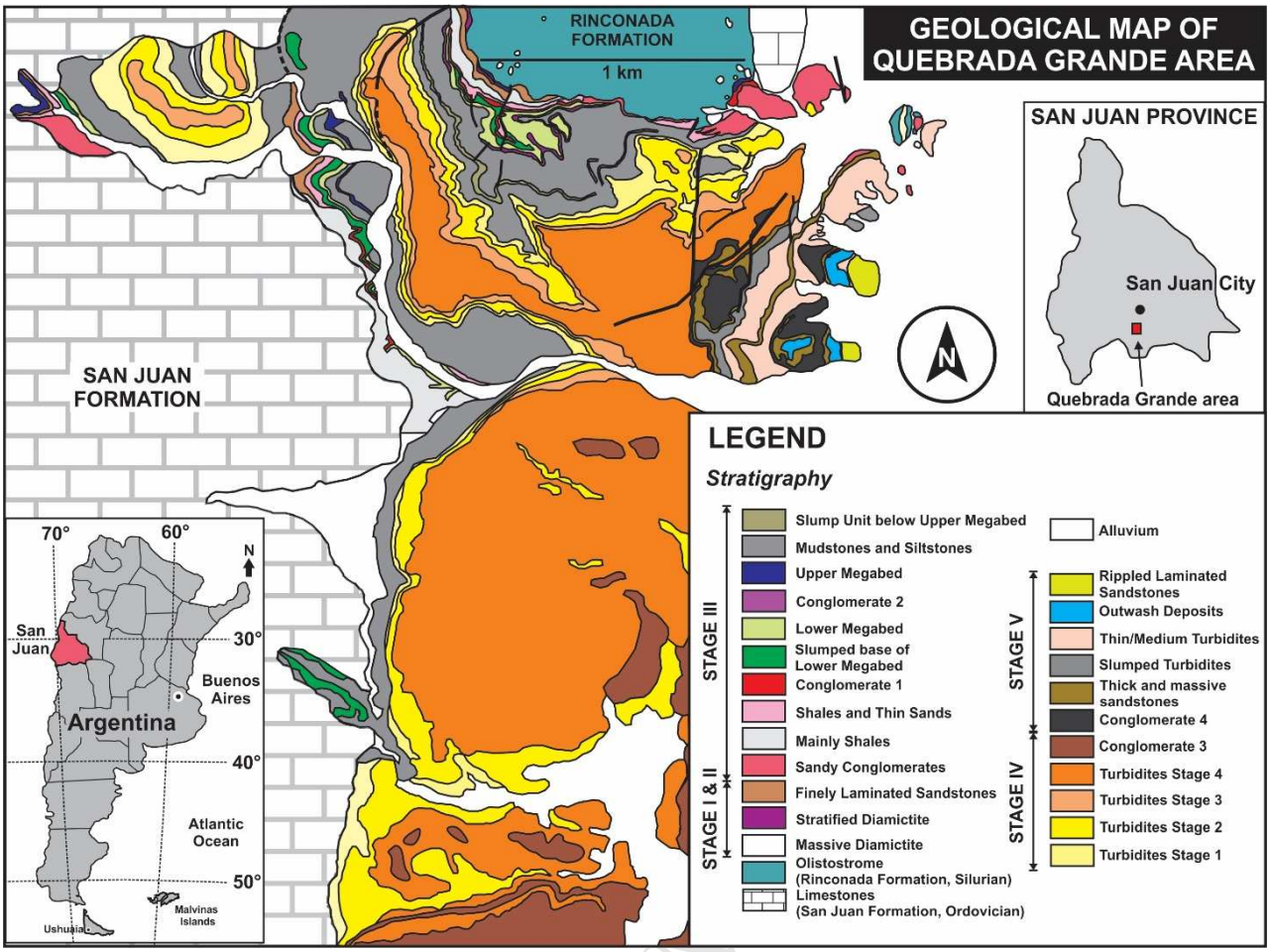

Figure 2

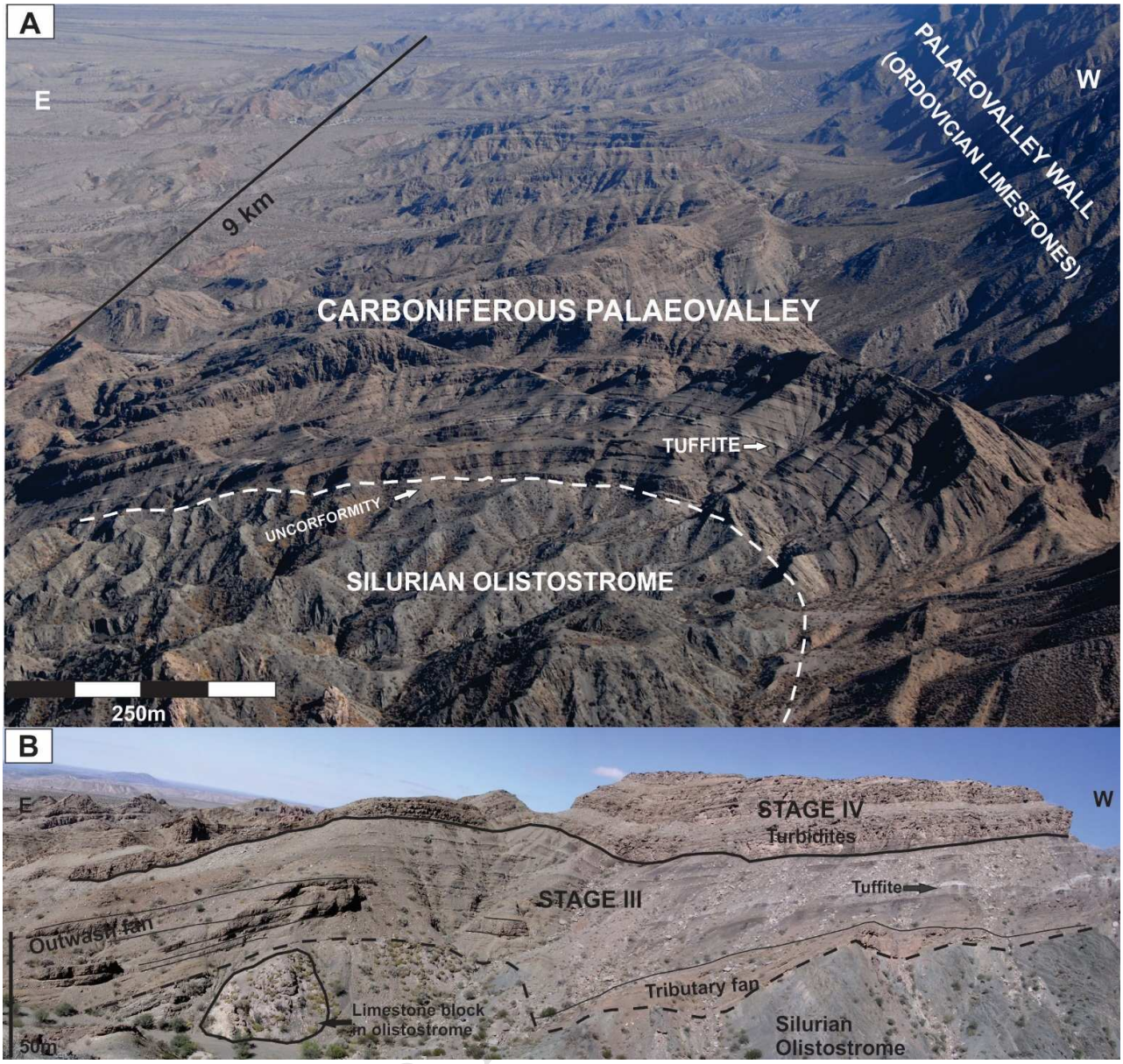

.

Figure 3

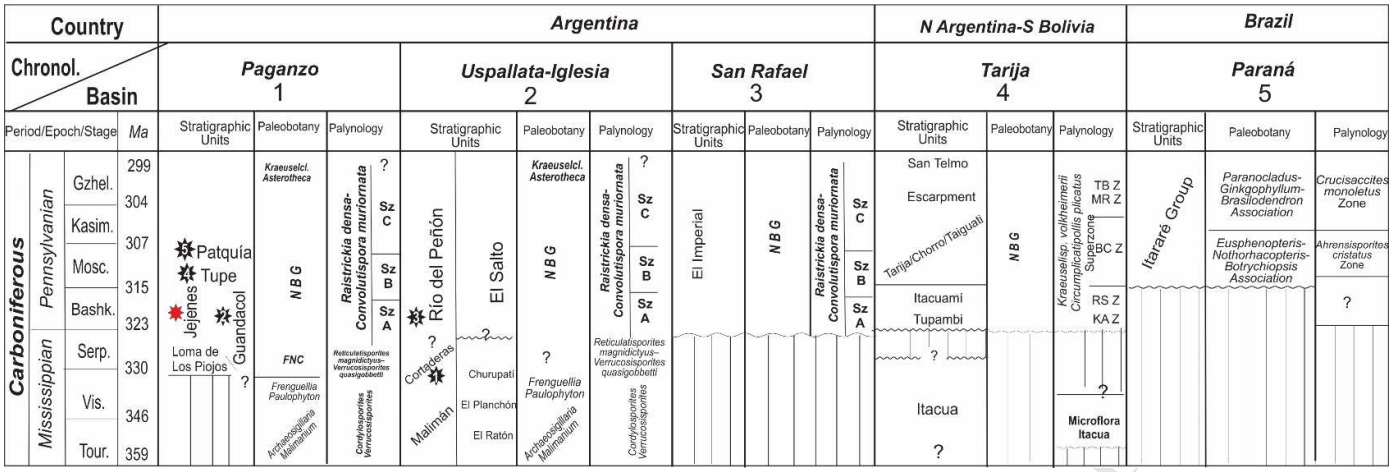

Figure 4

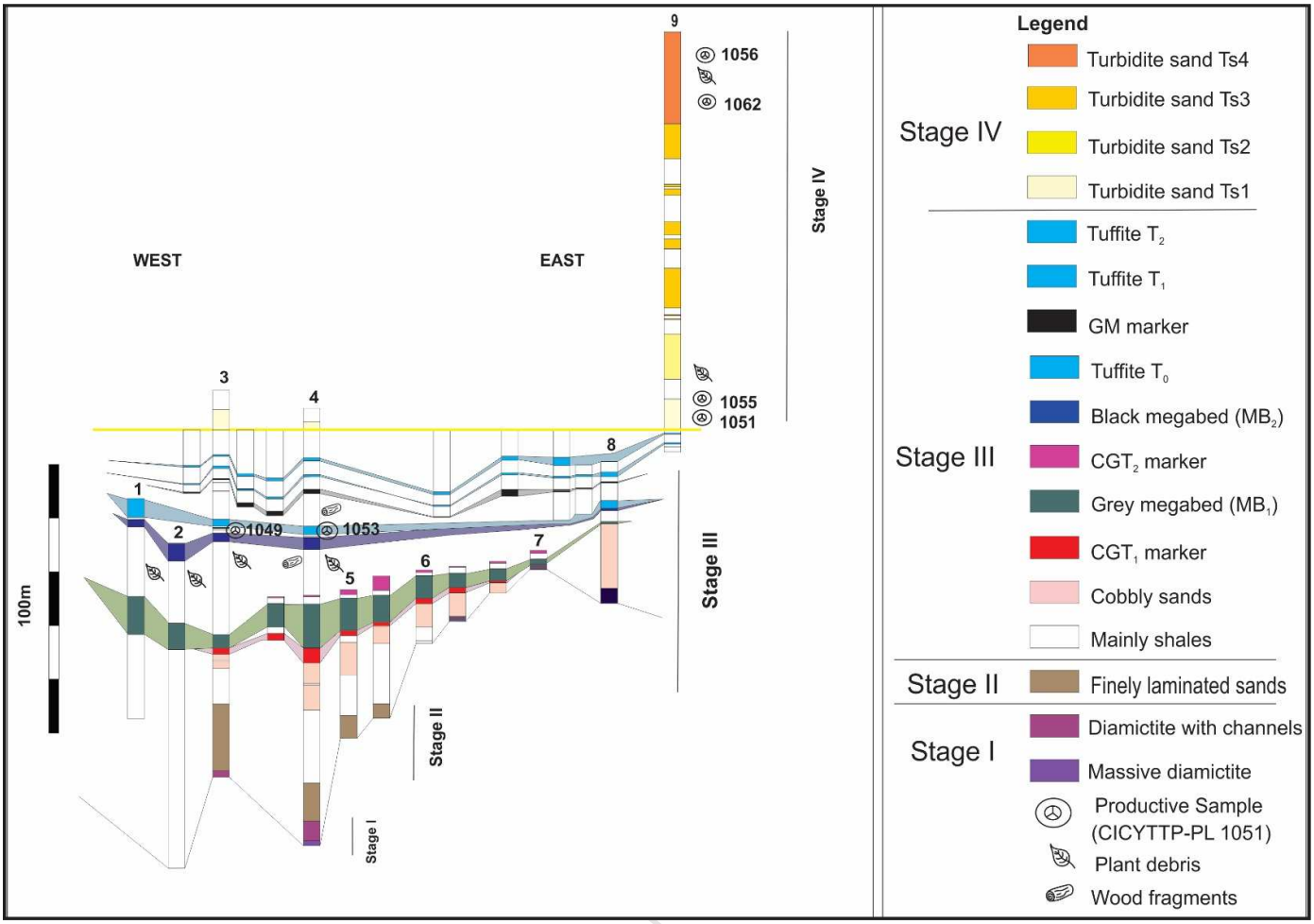

Figure 5

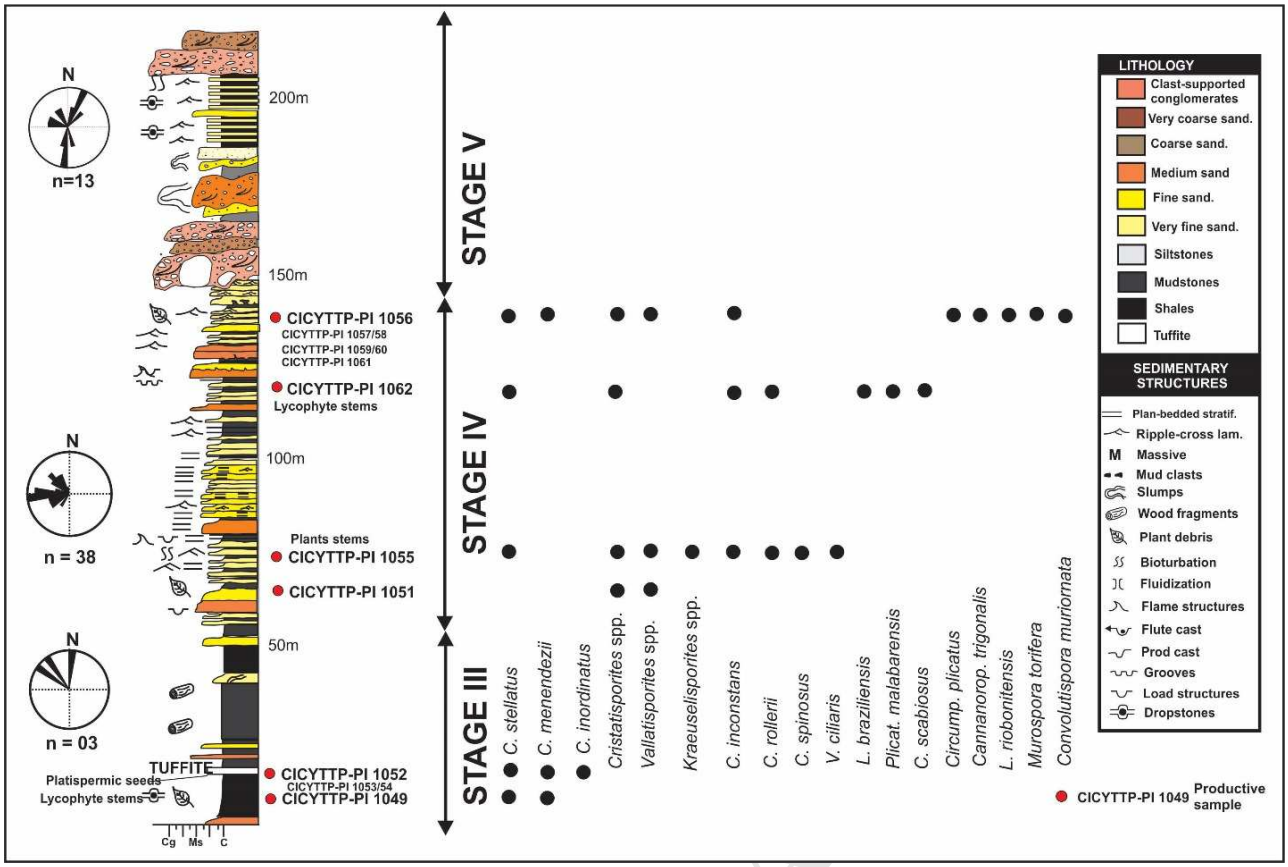

Figure 6

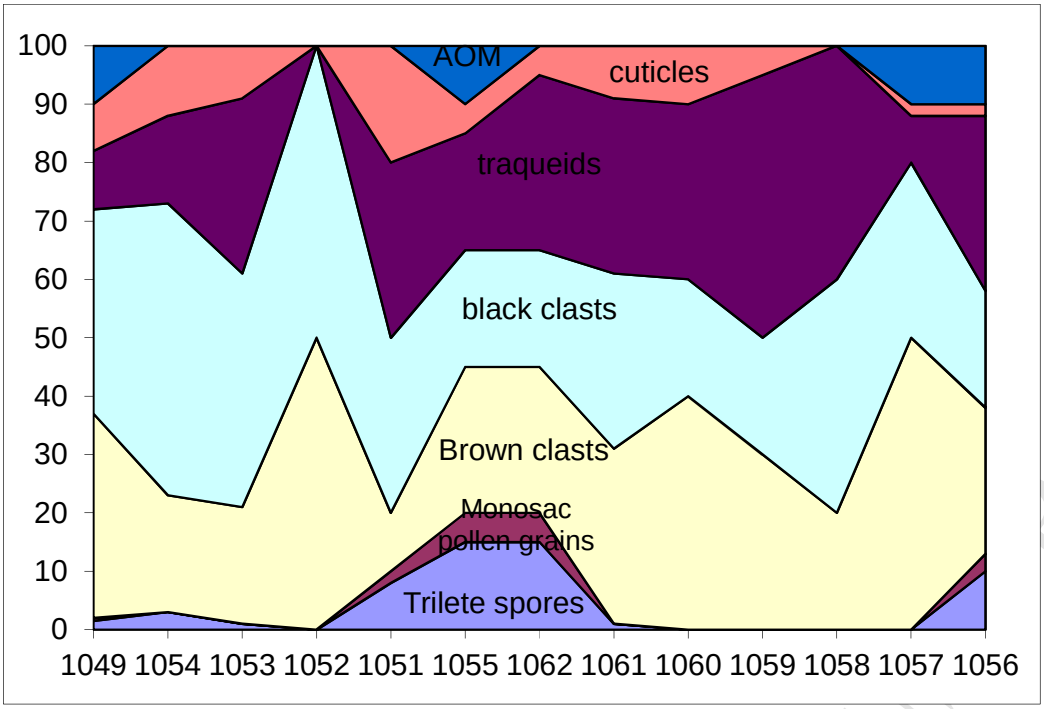

Figure 7

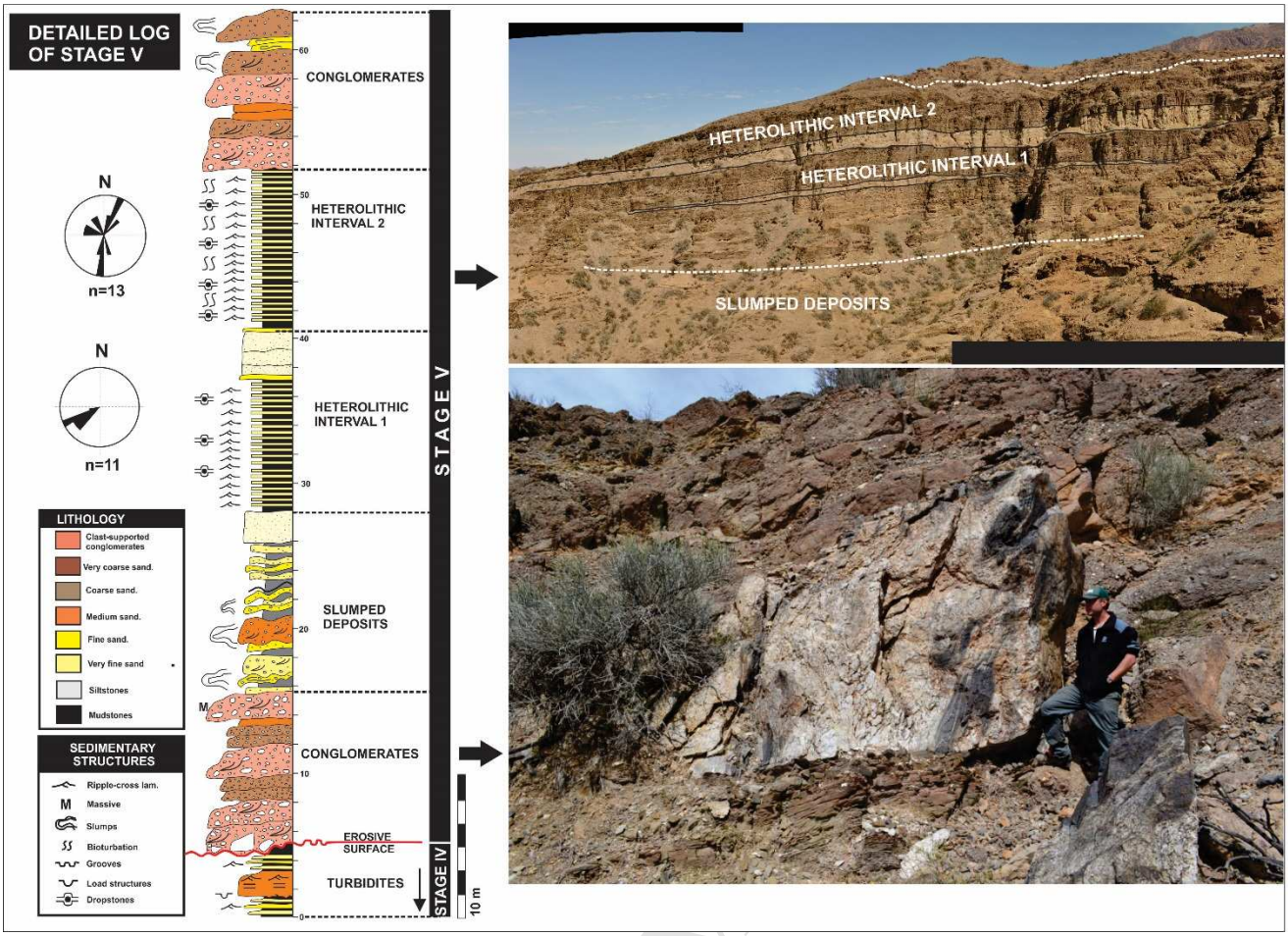

Figure 8

Figure 9

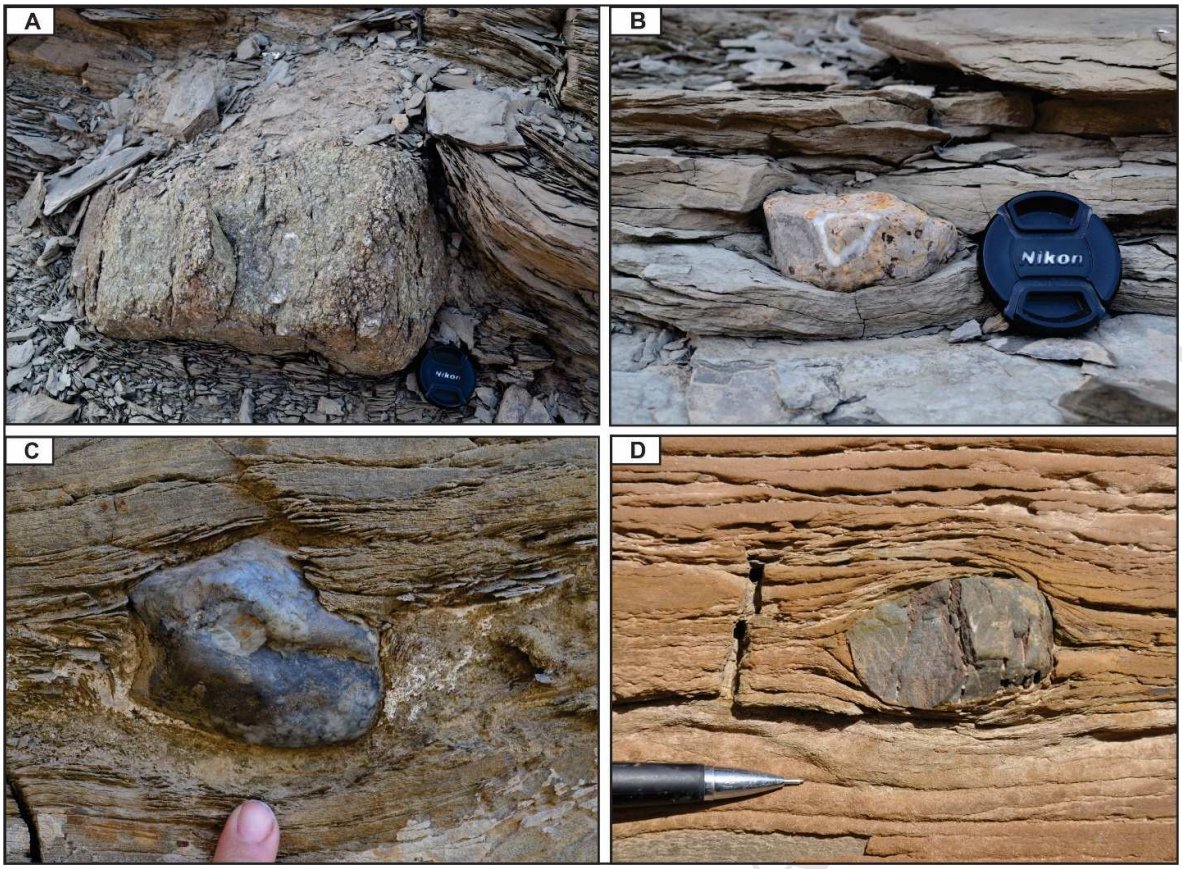

Figure 10

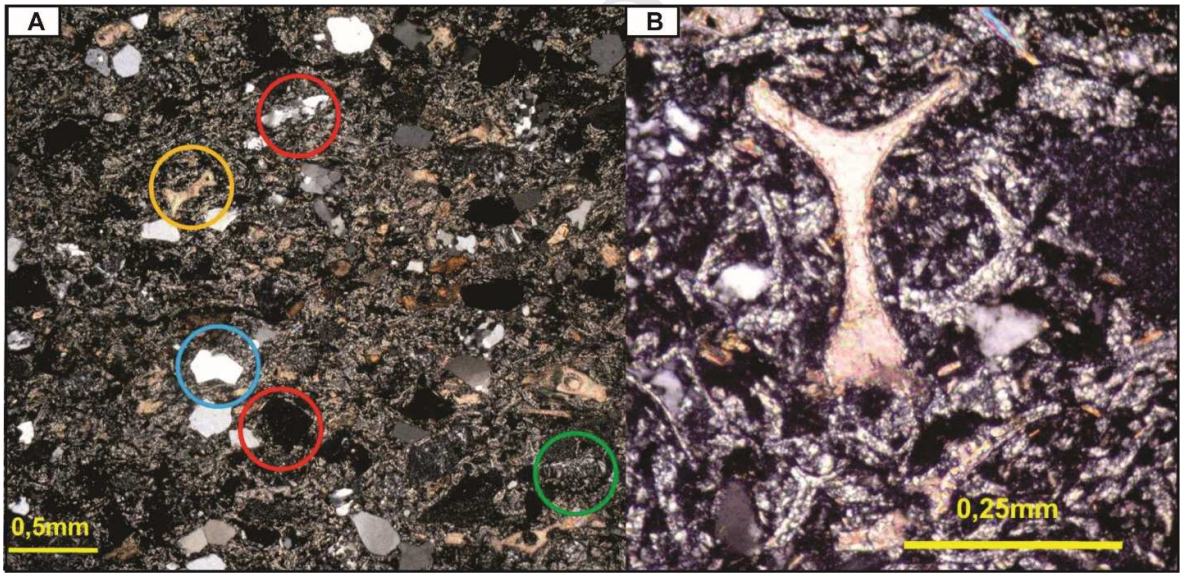

Figure 11

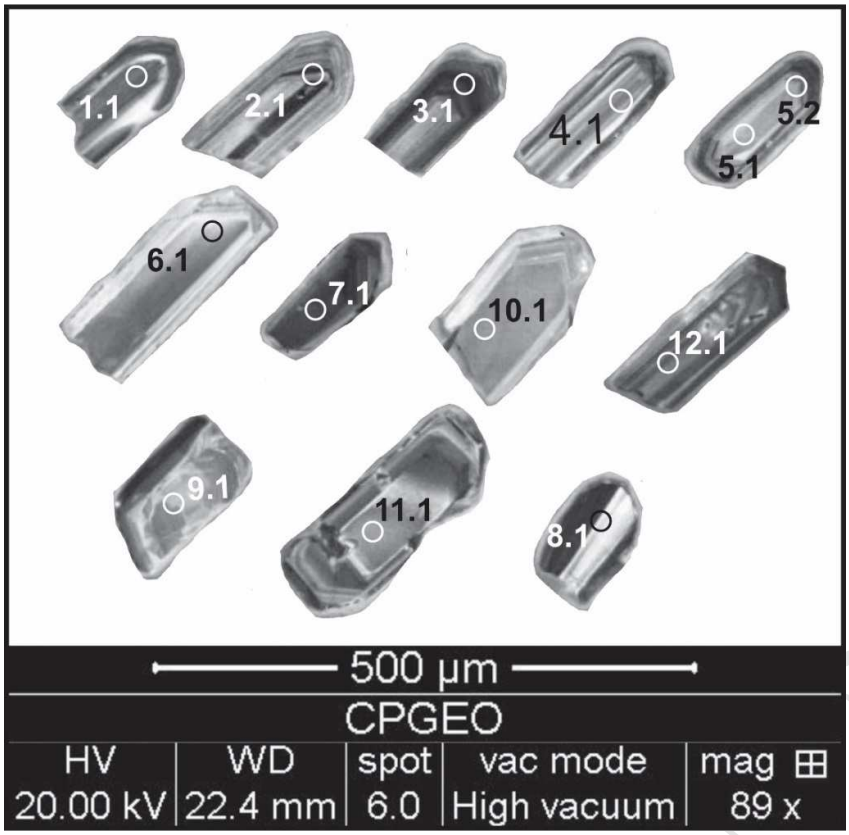

Figure 12

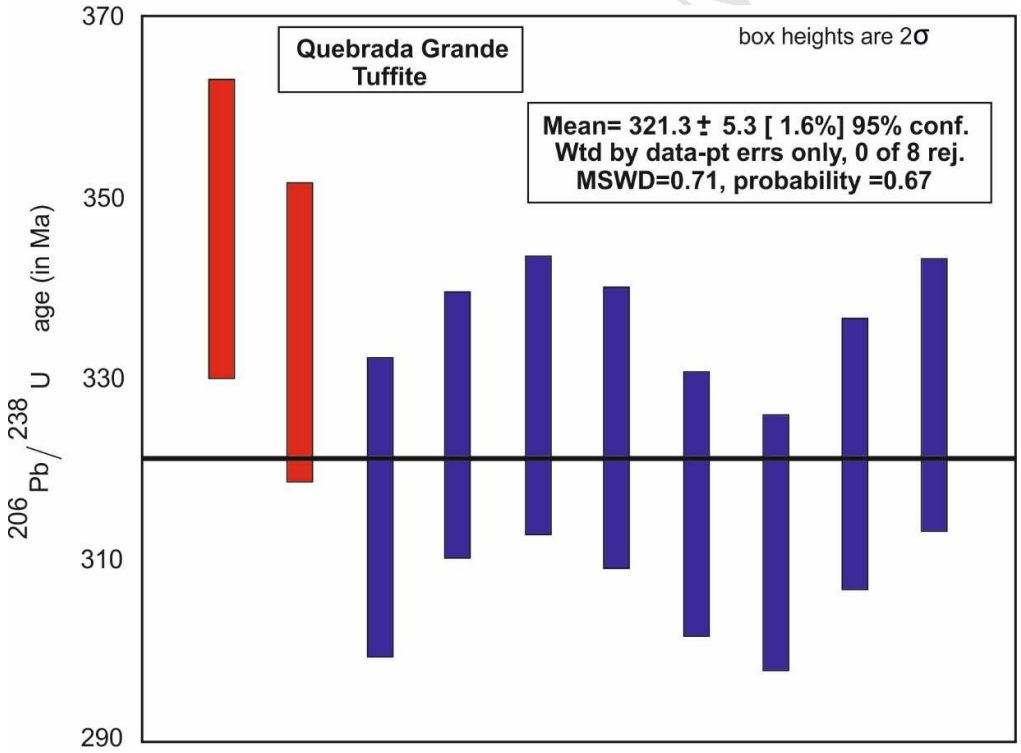

Figure 13

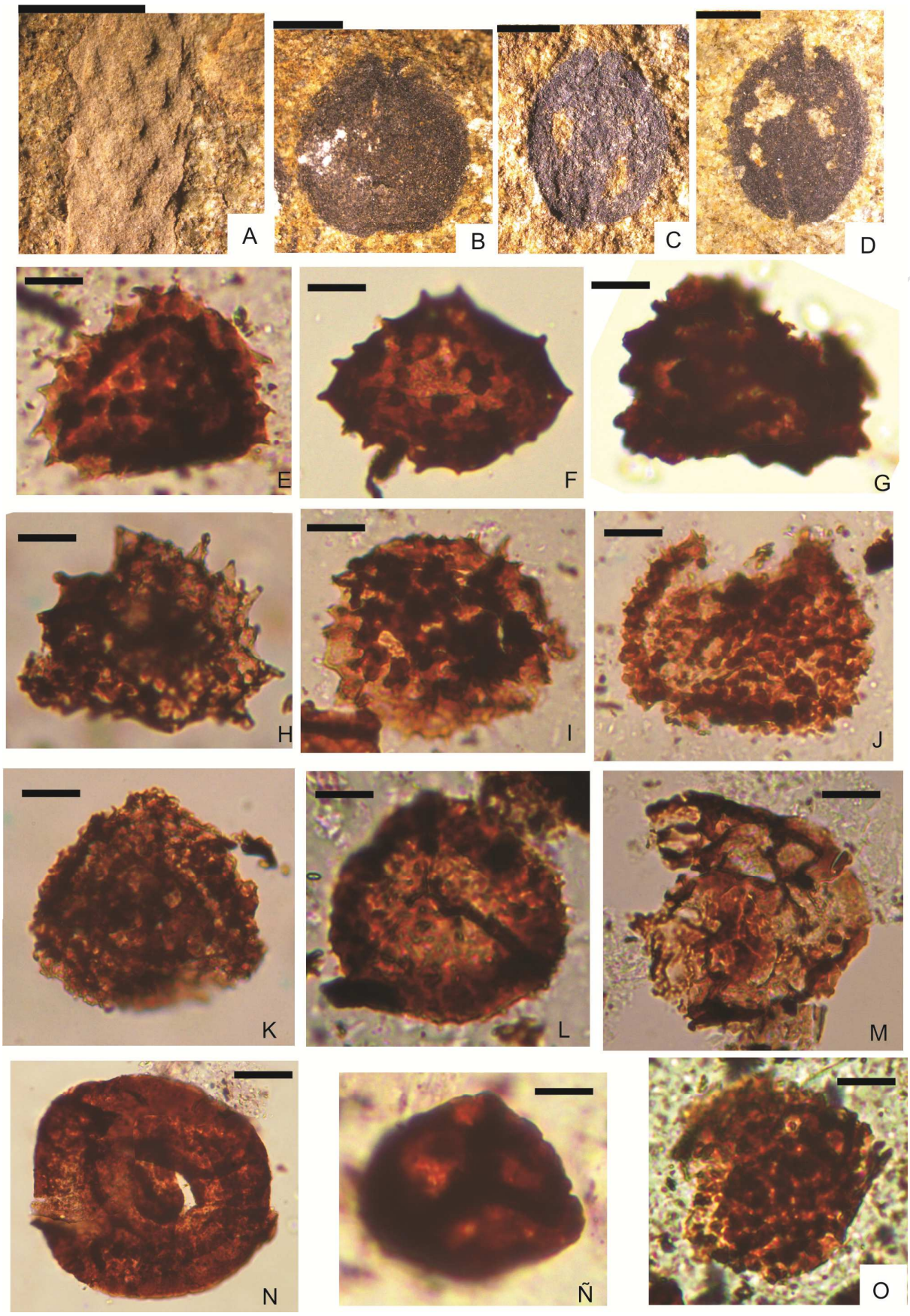

Figure 14

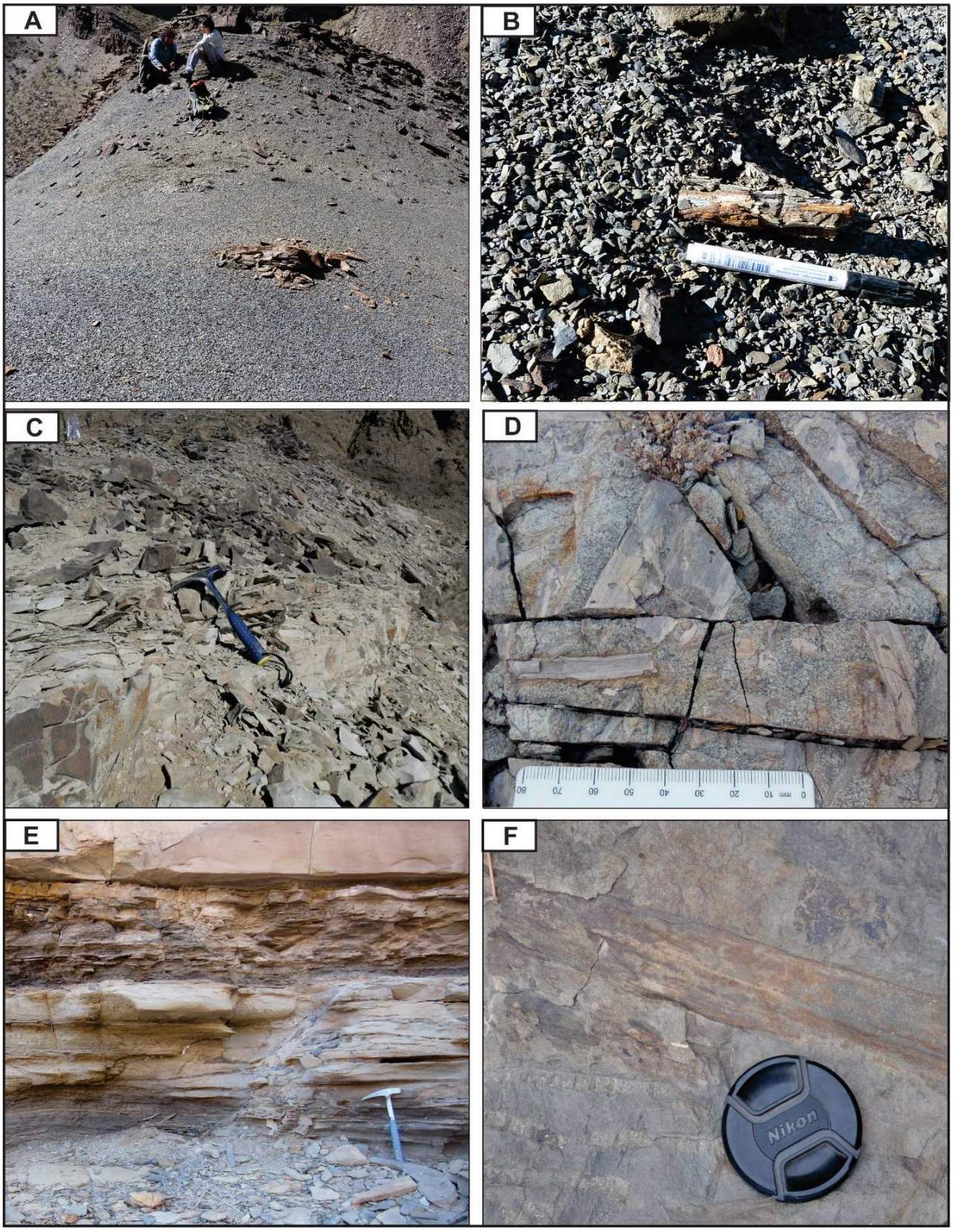

Figure 15

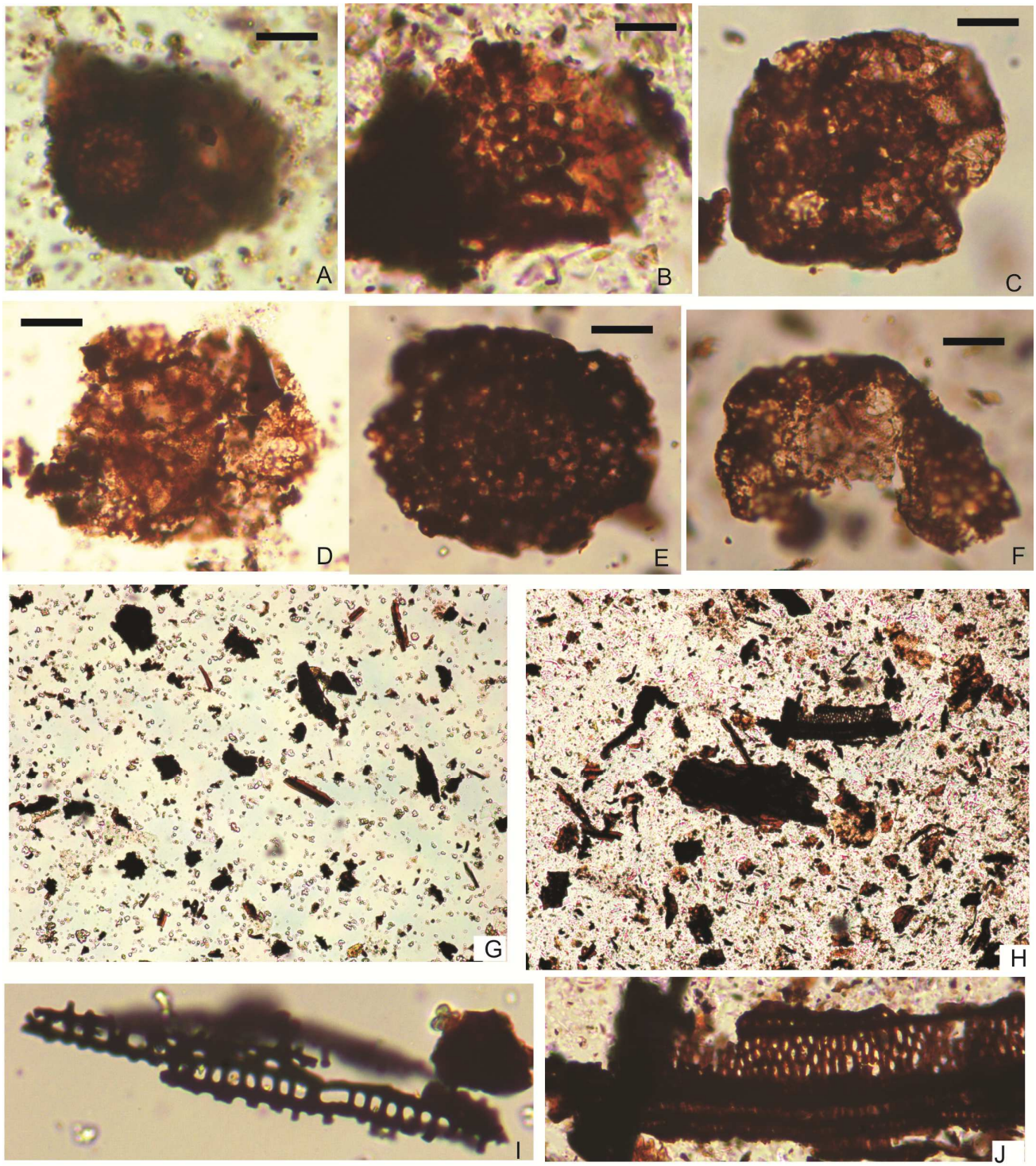

Figure 16

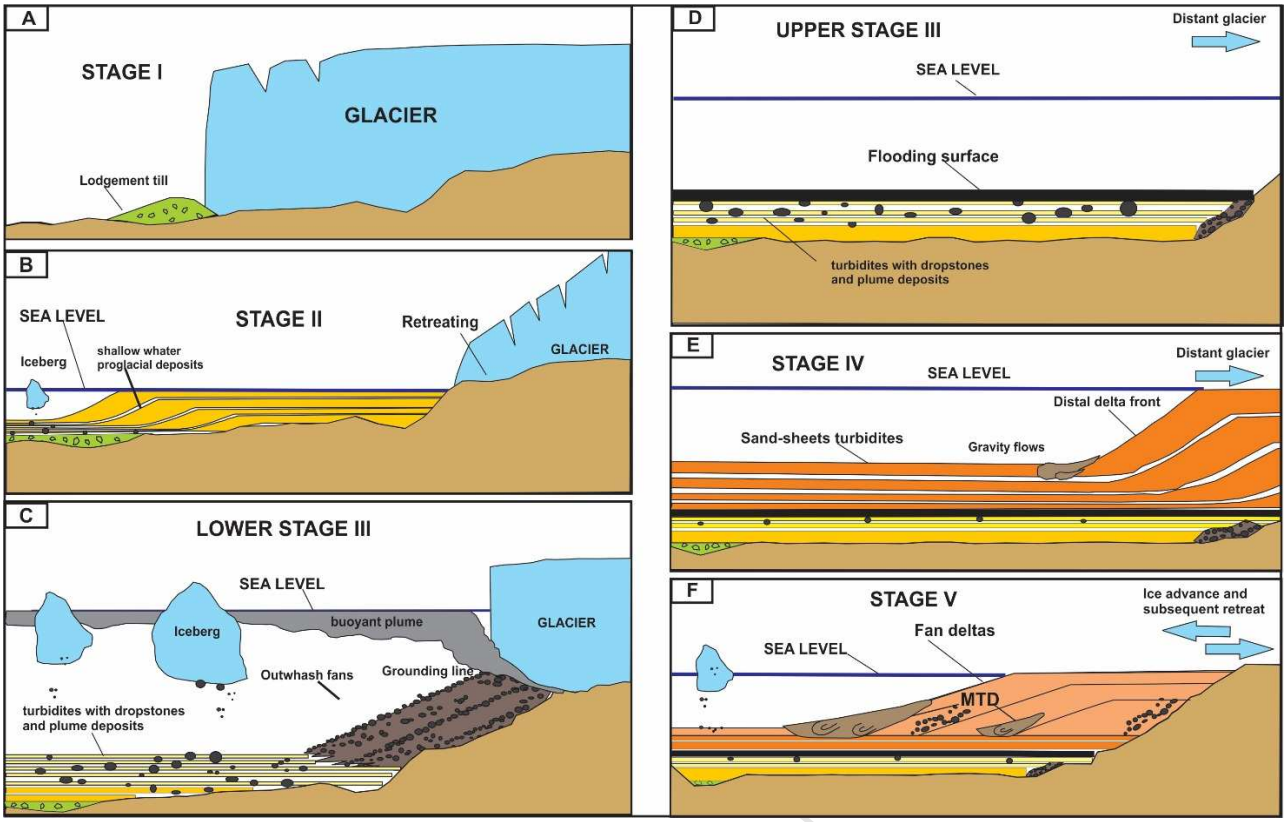

Figure 17

HIGHLIGHTS

- Age framework for the main Bashkirian transgression in Western Argentina.
- The first isotopic age for the Jejenes Formation.
- The first platyspermic seed for the region dated as 321.3 ± 5.3 Ma.
- A new glacial pulse recorded at upper section of Quebrada Grande palaeofjord.